BACTERIOGENICALLY INDUCED SULFURIC ACID ATTACK ON CONCRETE IN AN AUSTRIAN SEWER SYSTEM

Master thesis

By

Cyrill Grengg, BSc

Technical University Graz

Institute of Applied Geosciences

Supervisor

Prof. Dr. Dipl. Min. Martin Dietzel

Mag.rer.nat. Dr.rer.nat. Florian Mittermayr

Graz, June 2014

STATUTORY DECLARATION

I declare that I have authored this thesis independently, that I have not used other than the declared sources / resources and that I have explicitly marked all material which has been quoted either literally or by content from the used sources.

…… ……..
date (signature)

Acknowledgment

First of all, I thank my supervisors Prof. Dr. Martin Dietzel and Dr. Florian Mittermayr for their great support and special interest within my research and the constitution of this master thesis. Special thanks also to the staff of our laboratories, on whom I could always rely on when they were needed.

Furthermore, I want to thank all my classmates and friends for all the memorable and fun times which we were able to experience during numerous filed trips, journeys and the everyday life. I specially want to thank István, Peter and Klaus as being my closest friends and roommates, for their great input within my educational and private life during the last couple of years.

And finally, I thank my awesome family for their boundless support throughout my entire life.

Zusammenfassung

In dieser Masterarbeit wurde ein stark korrodiertes Kanalsystem intensiv über die Verknüpfung umfangreicher Kerngrößen untersucht. Ziel der Arbeit war die Gründe sowie den Ablauf der Korrosionsmechanismen für das verwendete Baumaterial zu verstehen, um in weiterer Folge Vorgaben für mögliche Restaurierungs- und Instandhaltungs- Maßnahmen geben zu können. Chemische und physikalische Parameter, wie pH Wert, Leitfähigkeit, Redox Potentiale und Temperaturen der Wasserphasen wurden vor Ort gemessen. Weiteres wurden Proben des Abwassers sowie Feststoffproben des korrodierten Materials entlang der gesamten Fließstrecke genommen. Im Labor sind Alkalinität, Konzentrationen gelöster anorganischer Inhaltsstoffe sowie des organischen Kohlenstoffgehalts bestimmt worden. Besonderer Fokus lag zudem auf mineralogischen Analysen des korrodierten Materials, wie Röntgendiffraktometrie, Rasterelektronenmikroskopie und Mikrosondenanalytik sowie Messungen zur Bestimmung der Kohlenstoff Komponenten und des Schwefelanteils im Feststoff. Des Weiteren wurden intensive Analysen in Bezug auf den Chemismus der Porenfluide durchgeführt. Auch sind die Konzentrationen von Schwefelwasserstoff (H_2S), Methan (CH_4) und Kohlendioxid (CO_2) in der Gasphase gemessen worden. Die Untersuchungen umfassten ferner die Messung der Verteilung der stabilen Isotope des Schwefels im gelösten Sulfat der Wasserphase und in den Porenfluiden des Betons, sowie im Schwefelwasserstoff in der Gasphase.

Aufgrund der Ergebnisse kann der Korrosionsmechanismus einer Reihe von komplexen chemischen Reaktionen zugeschrieben werden, welcher als „Micro biologisch induzierter Schwefelsäure Angriff“ bezeichnet wird. Im Verlauf dieses Prozesses wird über anaerobe Sulfat (SO_4^{2-}) Reduktion biogener Schwefelwasserstoff (H_2S) produziert. H_2S entgast in die Atmosphäre der betongesicherten Schächte, wo es in weiterer Folge in die äußeren Schichten des Betons diffundiert. Dort kommt es zu einer bakteriellen Rück-Oxidation, welche zur Bildung von Schwefelsäure führt. Diese reagiert mit den Zementphasen aus dem Beton, e.g. Kalziumhydroxid und Calcium Aluminat, was zu einer kontinuierlichen Auflösung der Zementphasen, sowie intensiver Bildung von Gips führt. Die diesbezügliche massive Betonzerstörung, kann innerhalb von wenigen Jahren zum kompletten Versagen des Kanalsystems führen.

Abstract

This master thesis comprises the application of a multi proxy approach, where a strongly deteriorated Austrian sewer system was intensively investigated .Various crucial parameters for detecting alteration features of the applied concrete were determined in the field and laboratory, including temperature, alkalinity, pH, and conductivity as well as distinct chemical analyses of the solution, respectively. Special focus was given on mineralogical analyses including scanning electron microscopy, X-ray diffraction measurements, as well as on total carbon/sulfur and microprobe analyses. Furthermore, intensive analyses of chemical compositions and parameters of the pore fluids were conducted, in order to gain better understanding of the thriving corrosive forces. Moreover, the concentration of gaseous hydrogen sulfide (H_2S), methane (CH_4) and carbon dioxide (CO_2) within the sewer pipe atmosphere was measured. Additionally, analyses of stable isotope signatures of sulfur in dissolved sulfate of the wastewater and the pore fluids of the damaged concrete as well as in the gaseous hydrogen sulfide were carried out.

The deterioration of the sewage system is attributed to a couple of complex reactions, which are referred to microbial induced concrete corrosion (MICC). Anaerobic, heterotrophic bacteria, present within the sewage systems, have consumed the organic matter, thereby reducing SO_4^{2-} to $H_2S_{(g)}$. Subsequently, degassing of the H_2S and its diffusion in the concrete lining, followed by its oxidation due to aerobic sulfur oxidizing bacteria occurred, thereby producing sulfuric acid (H_2SO_4). H_2SO_4 caused dissolution of the cementitious phases as well as gypsum formation, which finally caused the severe damage of the concrete within only several years.

Content

1 Introduction

Sewer systems had been a part of human culture since 7000 BC, where the first urban settlements were established [1]. Although ancient Rom was reported to operate a well-developed sewer network, no commonly used systems existed during the middle ages. With the time of the industrial revolution and thereby entailed growth of urban agglomerates, proper waste transport has been rediscovered to be an important part of modern society. Today we distinguish between three common types of sewer systems [2]:

Sanitary sewer networks:

Systems designed to collect and transport the daily sewage water of households and commercial areas, as well as of local industrial sites. The transported wastewater contains high concentrations of biodegradable organic matter and microorganisms, which results in biologically highly active environments. Therefore, chemical treatment within sewage purification plants is necessary, prior to injection into local receiving waters.

Storm sewer networks:

Systems built for water runoffs from urban areas i.e. streets, roofs or public sites, after precipitation events. The composition of meteoric water and drained solutions typically contains no or limited concentrations of biodegradable organic matter. Therefore, no or little chemical treatment is necessary before reinjection into local receiving waters.

Combined sewer networks:

Systems constructed to collect, mix and transport communal wastewater and urban runoff water. These systems operate like sanitary networks during dry periods, but possess the capacity to transport urban runoff waters during wet periods and storm events.

1.1 Sewer network – A complex system

It is inalienable to understand the chemical interaction between single phases within a sewer and their linkage to the physical properties of the system in order to construct sustainable

sewer networks and prevent possible corrosive effects. Therefore is important to distinguish between the physical parameters and chemical phases which interact within the sewer system. This chapter is designed to give a brief introduction into the characteristics of single important physical parameters i.e. design characteristics of the pipes, and the main phases present, seen from a chemical point of view.

1.1.1 Physical sewer parameter

The design characteristics and operation mode of sewer systems can be seen as the framework requirements which determine, to a great extent, the possible processes within the system. I. e. the presence of power mains, their length and aperture, as well as construction materials and pump rates represent the set-up of the system in which the processes proceed [2]. The following examples constitute the reciprocal effects between design and operation characteristics with consequential conditions for sewer processes.

The retention time and water depth of the wastewater flow influences the re-aeration and thereby the occurrences of aerobic, anoxic and anaerobic conditions within sewer networks, which is crucial for the type of microbiological oxidation of organic matter.

The flow velocity and pipe diameter have huge impact on the built up and deposition of sediments and biofilms along the sewer walls which again determines the living environment of possible bacterial colonisation.

Flow mechanisms and turbulences influence the release of toxic and malodourous gases into the sewer atmosphere as well as the re-aeration rate of the wastewater.

1.1.2 Chemical and microbial processes

From the chemical point of view a sewer can be seen as a “reactor for chemical and microbial processes” [2] in which reactions and interactions occur in and between one or more of the five phases present: the wastewater phase, the biofilm, the deposits, the sewer atmosphere and the sewer walls.

Figure 1 Figure 1 illustrates the dynamic interaction between the sewer phases and their receiving surrounding environments.

In order to understand the course of chemical and biological actions within sewer systems it is central to understand the redox conditions present within the system. Reduction and Oxidation of substances play an important role within microbiological driven biodegradation. In this context the chemical composition of the transported wastewater is a key factor concerning possible reactions. The availability of different electron acceptors i.e. dissolved oxygen (O_2), nitrate (NO_3^-) and sulfate (SO_4^{2-}), control the course of action within the redox system. Consequently, this has a huge impact on potential sewer corrosion as well as production and ventilation of toxic and malodourous gases.

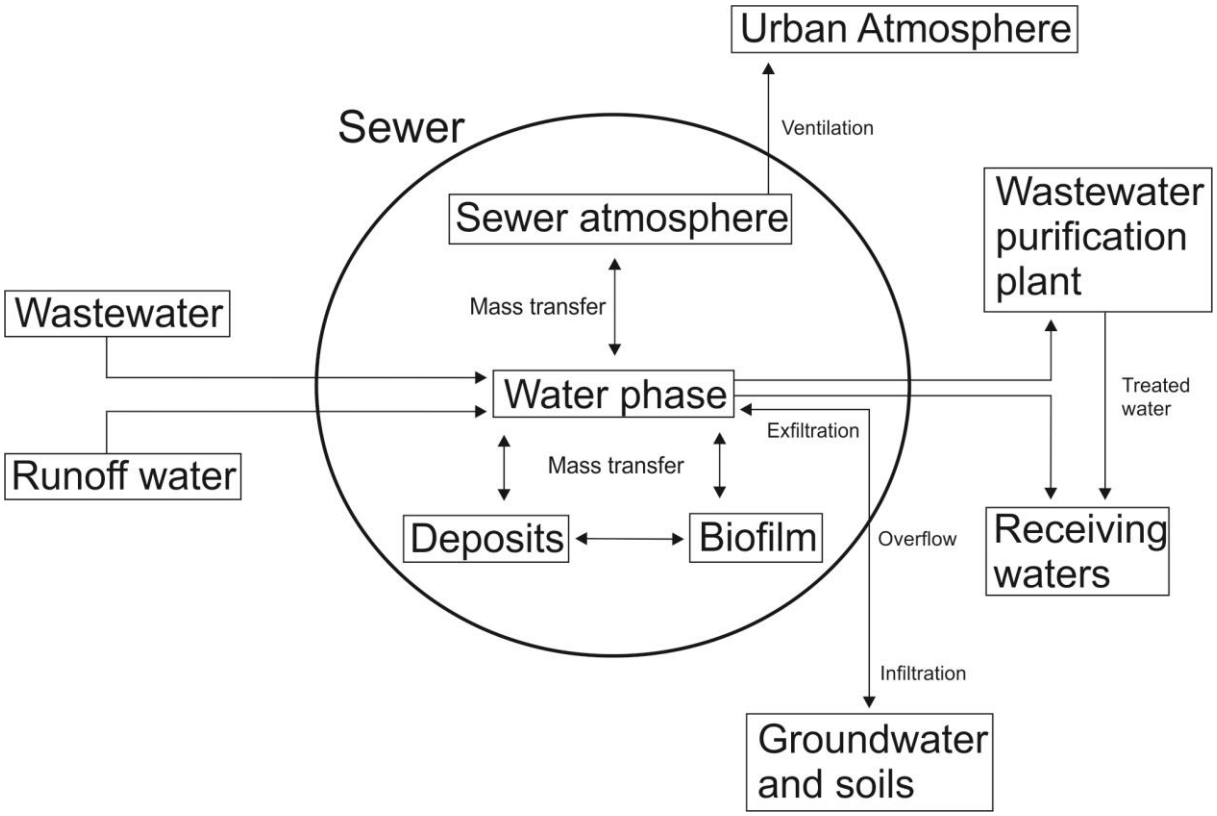

Figure 1: Schematic illustration of interaction between the five phases present within a sewer system. Arrows indicate the possible mass transfer between the phases present within the sewer and its receiving surrounding environments (modified after [2]).

2 Sulfate attack on concrete

Concrete is a multiphase, porous, strongly basic material [3], which is often exposed to aggressive aqueous environments. Due to the contact with groundwater, soils or wastewater sulfate attack is one of the major reasons/triggers for structure failure, causing huge remediation costs worldwide [4-6]. Beside water, as being an essential participant in the chemical reactions, the chemical composition and physical parameters of the cementitious matrix are crucial in determining the reaction mechanisms [3]. The chemical reactions can be sub classified into two subcategories: The dissolution of the hydrated and non-hydrated cementitious phases and/or precipitation of newly formed products [3]. Physical parameter such as pore networks, distributions and connectivity of capillary porosity also play a significant role for secondary chemical reactions, since diffusion and permeation are two of the key mechanisms for the transfers of materials [3]. Generally said there are two main mechanisms describing sulfate attack on concrete.

(i) External sulfate attack comprises sulfate from surrounding sources, e.g. wastewater or soils, which is transported into the pore volume of the concrete. Subsequently, chemical reactions between the sulfate and the cementeous phases of the concrete occur, resulting in formation of newly formed sulfate salts with significantly higher specific volumes [6, 7], i.e. gypsum, ettringite, compared to the educts, i.e. calcium hydroxide, calcium aluminates. The formation of the volume expansive products causes stress ensuing cracking of the concrete. At the same time gypsum and ettringite hold low internal strength, thereby significantly reducing the tensile strength of the concrete. Furthermore, the saturated conditions with reference to H_2O cause leaching and gradual removal of the latter products.

(ii) Internal sulfate attack can be mainly attributed to delayed ettringite formation (DEF), although oxidation of primary sulfide within the cementeous composition, thus increasing sulfate concentrations is also referred to the same matter [3]. DEF is a process where spontaneous physical expansion occurs, due to an isochemical process in which the distribution of sulfate changes and ettringite forms. Whereas this process occurs volitional during the early stages hardening of diverse concrete structures and thereby compensating for chemical shrinkage [8], it decreases the internal strength of the concrete significantly when proceeding during the DEF [9, 10].

2.1 Microbial induced concrete corrosion (MICC)

MICC represents a sulfate related attack, where the life span of concrete structures can be reduced to less than a decade [11]. It is attributed to in-situ production of sulfuric acid due to a chain of complex chemical reactions, caused by bacteriogenic activity. Sewer systems with slow flowing wastewater or low pump rates favor the formation of sediment deposits and biofilms along the sewer walls. Due to bacterial oxidation from organic matter depletion of dissolved oxygen (O_2) and nitrate (NO_3^-) within the wastewater occurs. Subsequently, anaerobic conditions prevail and sulfate (SO_4^{2-}) is used by strains of sulfate reducing bacteria, i.e. Desulfovibrio, as electron acceptor, thereby producing hydrogen sulfide (H_2S). Thereupon, degassing of H_2S into the sewer atmosphere occurs. The physical and environmental parameters liable for sulfide production are described in section 1.1.1 and 2.1.1. H_2S diffuses into the outer layer of the concrete and serves as an energy source for different families of sulfide oxidizing bacteria. The bacterial colonization of the concrete pore volume is progressive, since different families of bacteria thrive best at different pH levels [12]. The final product is sulfuric acid (H_2SO_4) which attacks the cementitious paste of the concrete. Dissolution of the primary cementitious phases, mainly portlandite ($Ca(OH)_2$) and calcium-aluminate phases and formation of sulfate salts, mainly gypsum ($CaSO_4 \cdot 2H_2O$) and ettringite ($(CaO)_3 \cdot Al_2O_3 \cdot (CaSO_4)_3 \cdot 32H_2O$) proceed, according to the overall reactions below [6].

$$CaO \cdot SiO_2 \cdot 2H_2O + H_2SO_4 \rightarrow CaSO_4 + Si(OH)_4 + H_2O \quad \textbf{Equation 1}$$

$$H_2SO_4 + CaCO_3 + 2H_2O \rightarrow CaSO_4 \cdot 2H_2O + H_2CO_3 \quad \textbf{Equation 2}$$

$$H_2SO_4 + Ca(OH)_2 \rightarrow CaSO_4 \cdot 2H_2O \text{ (gypsum)} \quad \textbf{Equation 3}$$

$$3CaSO_4 \cdot 2H_2O + 4CaO \cdot Al_2O_3 \cdot 13H_2O + 14H_2O \rightarrow (CaO)_3 \cdot Al_2O_3 \cdot (CaSO_4)_3 \cdot 32H_2O \text{ (ettringite)} \quad \textbf{Equation 4}$$

These sulfate salts have significantly higher specific volumes than the primary cement phases, which causes internal cracking according to internal and external sulfate attack, described in section 2.

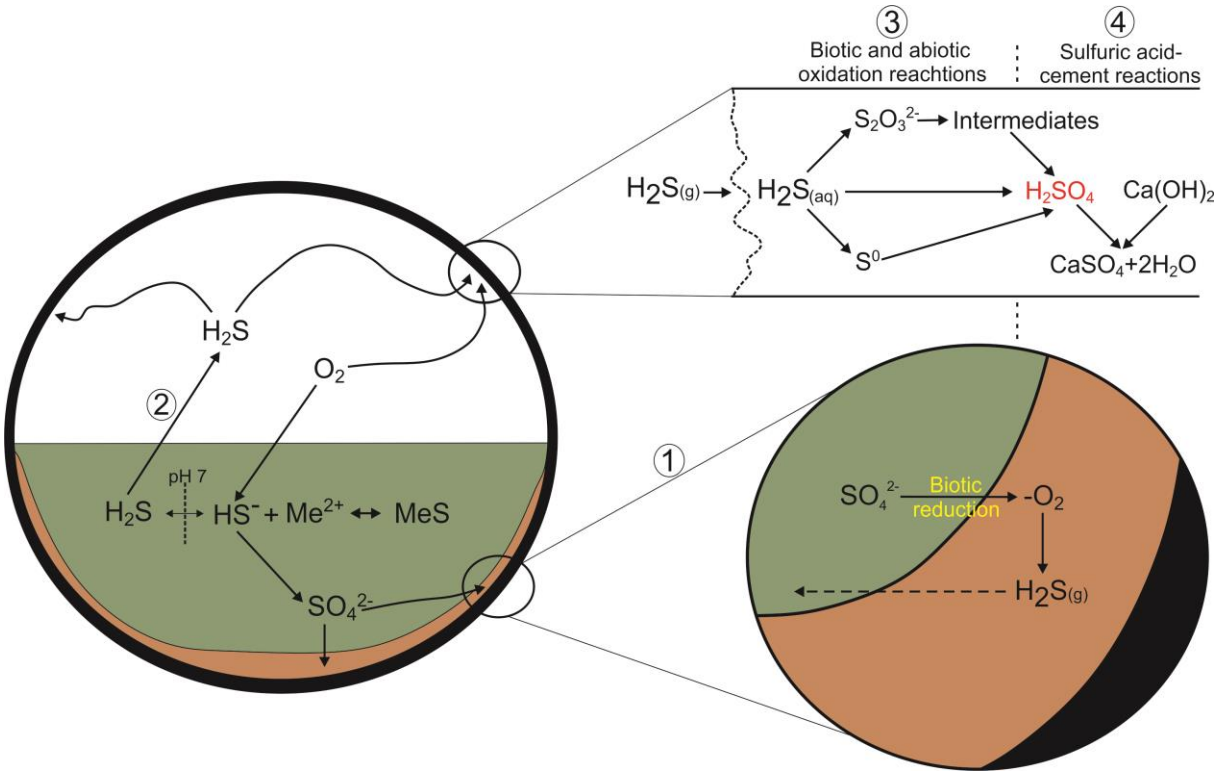

Figure 2: The sulfur cycle within sewer systems. Initial reduction of sulfate (SO_4^{2-}) occurs within the anaerobic biofilm producing H_2S (1), followed by degassing into the sewer atmosphere (2) and diffusion into porous surfaces of the concrete. There, oxidation of H_2S with the final product of sulfuric acid (H_2SO_4) proceeds (3), which is reacting with the cementitious phases of the concrete to form gypsum ($CaSO_4 \cdot 2H_2O$) (4). Also illustrated is the pH dependency of sulfide species and possible reactions of dissolved hydrogen sulphide ions with occurring metal ions (Me).

2.1.1 Limiting environmental and chemical conditions of MICC

Environmental factors and chemical conditions play an essential role during the formation and propagation of MICC. Especially during the early stages of the corrosion, change in pH, temperature or concentrations of H_2S, determine the course of action [4]. This chapter seeks to summarize the most important environmental and chemical factors, which control the intensity and rate of biogenically induced concrete corrosion.

The pH within the system determines the distribution of sulfide species within the wastewater, thus influencing, to a great extent, the production and emission of gaseous H_2S. Additionally, the concrete surface pH dictates the propagating colonization of sulfide oxidizing bacteria within the pore volume of the concrete [13].

The activity of the bacteria is highly influenced by prevailing temperature conditions. The activity of sulfate reducing (SRB) and sulfide oxidizing (SOB) bacteria doubles with increasing temperatures of 10 °C [14], reaching a maximum at 30 °C [15].

High relative humidity is needed in order to engage in the solving part of the MICC, thereby ensuring the evacuation of the dissolved cementitious phases. Also, the formation of corrosion products, i.e. gypsum and ettringite, requires wet conditions.

The composition of the concrete and especially its pore volumes represent the growing environment of the SOB. High porous concrete increases the living environment of SOB, thus favoring high colonization rates entailing high production rates of sulfuric acid. Also the propagation and diffusion of damaging components is alleviated with increasing pore structures.

2.1.2 Chemical parameters of H_2S

Hydrogen sulfide (H_2S) appears under standard conditions (1 atm/20°C) as a colourless, flammable gas, with an explicit malodour, similar to rotten eggs and a density higher than air. Its chemical structure is similar to water (H_2O), although due to the difference in size between the sulfur and the oxygen atom, H_2S shows lower polarity. Therefore no hydrogen bonds between the molecules are occurring [16]. It is chemically very reactive, degrading in the atmosphere thereby forming H_2O and SO_2 within several days [17]. Generally, the threshold for smelling ranges around 0.0005-0.3 ppm, however at high concentration a person might lose their ability to smell it, which makes it very dangerous to human health. Exposure to low concentration of H_2S might lead to eye, nose or throat irritations. Higher concentrations can generate unconsciousness causing death when longer exposed. Typical threshold values are shown in Table 1.

Table 1: Main thresholds of H_2S on human beeings [17].

Hydrogen Sulfide $(H_2S)_{(g)}$ in [ppm]	Ramifications
>0.00047	Odor threshold for human beings
10-20	Eye irritations; Headache
50-100	Damages of eyes/ respiratory system/ tussive irritation
>100	Emerging odorlessness for human beings
300-500	Pulmonary oedema / possible death
>700	Immediate death

Within an aqueous solution H_2S behaves like a weak, dibasic acid, which gets dissociated in a first step to dissolved hydrogen sulfide (HS^-) and finally to sulfide ion (S^{2-}) [16]. This pH depending distribution is shown in Figure 3.

$$H_2S + H_2O \leftrightarrow H_3O^+ + HS^- \qquad pKs = 7.0 \qquad \textbf{Equation 5}$$

$$HS^- + H_2O \leftrightarrow H_3O^+ + S^{2-} \qquad pKs = 12.9 \qquad \textbf{Equation 6}$$

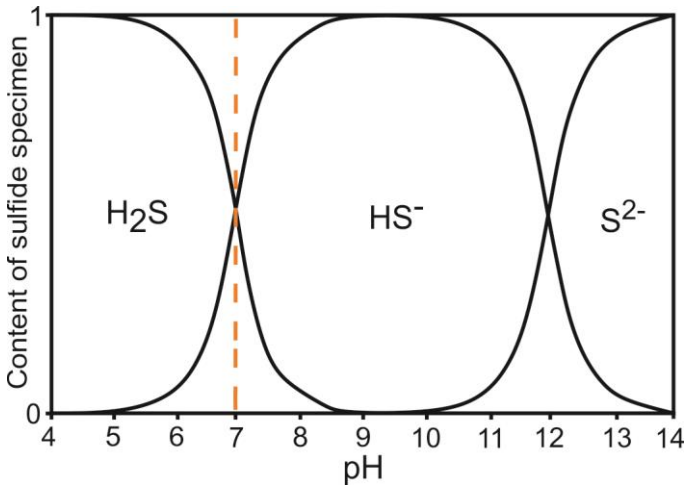

Figure 3: Showing the distribution of sulphide specimen with pH at 25°C (modified after [13]).

2.2 Isotope fractionation

Isotopic analyses have proven to be a value tool for all kind of different areas of research. In environmental sciences there exists a wide spread field of applications e.g. climate researches, quality control or age dating, to name only a couple of them. To the authors knowledge so far no isotopic study had been conducted, describing the microbial processes within sewer systems which are affected by MICC.

Generally said isotopes are defined as atoms that exist at different variants with the same number of protons but different number of neutrons. This difference in mass between single isotopes concludes different physical parameters which are referred to as isotope effects. Isotopes can be separated into groups of stable and unstable (radioactive) isotopes, whereas the overwhelming majority are unstable with over 1200 discovered isotopes. At the same time around 300 known stable isotopes exists, although the term "stable" is relative, depending on the detection limits of radioactive decay times [18]. Isotopic compositions within one system are generally noted as delta (δ) values:

$$\delta_A = (ratio_A / ratio_{st} - 1)\ 10^3\ (‰) \qquad \textbf{Equation 7}$$

where $ratio_A$ represents the measured isotope ratio and $ratio_{st}$ is that of the defined standard of the given system [18]. The difference in isotopic compositions between two systems, i.e. wastewater and pore fluids, due to isotopic exchange is defined as isotopic fractionation. Consistently, the fractionation factor (α) represents the ratio of two isotopes within one chemical compound (A) divided by the corresponding ration for another chemical compound (B) [18] and is expressed in $\alpha_{A-B} = ratio_A / ratio_B$

Equation 8:

$$\alpha_{A-B} = ratio_A / ratio_B \qquad \textbf{Equation 8}$$

In general isotopic fractionation can be subcategorized into equilibrium and kinetic fractionation. Equilibrium fractionation is defined as the partial separation of isotopes between substances at isotopic equilibrium due to differences in vibrational energy, i.e. evaporation and condensation sequences [18]. Kinetic fractionation occurs due to different reaction rates of isotopic molecules [18], i.e. biogenic fractionation occurs due to the affinity of organisms to incorporate the "lighter" isotope within their body structure.

3 Field study

3.1 Introduction

Corrosion of concrete based sewer systems due to the emission of hydrogen sulfide (H_2S) from wastewater is a huge economical factor and worldwide occurring issue. The so-called microbially induced concrete corrosion (MICC) [19] can reduce the lifespan of concrete structures, from expected 100 down to 30-50 years, in extreme cases even down to 10 years [20]. The required remediation are challenging and generate high costs worldwide. It is calculated that the United States is going to spend 390 billion dollar within the next 20 years in order to maintain the existing wastewater infrastructure [21]. In Los Angeles County in 1996 over 400 billion Euro were spend for restorations of corroded sewer systems which can be directly assigned to MICC [4]. Moreover, hydrogen sulfide and other volatile components i.e. ammonium (NH_3) are extremely toxic with significant health related consequences [16, 17]. Although the earliest studies of MICC date back to 1900 [22] parts of the mechanisms are still in debate.

The deterioration of the concrete is attributed to a chain of complex chemical, abiotic and biotic reactions. Sulfate reducing bacteria (SRB), mainly of the genus Desulfovibrio spp. and Desulfomaculum spp. [13], present in the anaerobic biofilm and sediments of the sewer walls break down organic matter, thereby reducing sulfate into gaseous hydrogen sulfide (H_2S) [3]. Subsequent degassing of hydrogen sulfide (H_2S) into the sewer atmosphere occurs, followed by its diffusion into the pore volume of the concrete. Initially, since concrete is a strongly basic material with initial pH around 13, chemical acid-base reactions with carbonation (CO_2) and H_2S acidification causing the pH to drop. Starting from pH around 9.5 progressive colonization of species of sulfur oxidizing bacteria occurs, which use H_2S either directly [12] or over different key precursors e.g. Thiosulfate (S_2O_3) or elemental sulfur (S^0) as an electron donor. The final product is biogenic sulfuric acid (H_2SO_4) which attacks the concrete [23] and leads to its dissolutions, as well as mineralogical transformations of the alkaline components of the cementeous paste. The main products are gypsum ($CaSO_4 \cdot 2H_2O$) and ettringite ($(CaO)_3 \cdot Al_2O_3 \cdot (CaSO_4)_3 \cdot 32H_2O$), which both hold low structural strength and significant higher specific volumes than the cementitious phases, thereby weakening the concrete [6]. The formation of the expansive products is believed to cause internal cracking, thus exposing new surface areas to acid attack. With advancing decrease in pH different strains of bacteria

adopt the pore volume, with Acidithiobacillus Thiooxidans being the most aggressive one [3]. Acidithiobacillus T. thrive best at pH around 2 but being capable of surviving pH as low as 0.2 [24].

While many laboratory studies have been carried out focusing on the effects of MICC on different types of concrete [7, 19, 25, 26], so far only few data of field studies exist [27]. Although various conclusions and significant findings could be and can be concluded from laboratory analyses, it is almost impossible to simulate completely equivalent environmental conditions. This paper comprises the application of a multi proxy approach, where a strongly deteriorated Austrian sewer system was intensively investigated. It aims to describe one bacteriogenically induced sulfuric acid corrosion sequence, its factual reasons, processes and catalysts as well as the corrosive consequences on concrete within one field study. Besides of chemical and mineralogical analyses of the solid and liquid phases throughout the system, intensive analyses of chemical compositions and parameters of the concrete pore fluids were conducted. Furthermore, bacteria analyses were carried out and gas concentrations were measured. The results comprise a consistently described case study of an extremely fast progressing MICC, giving new insights on the reaction mechanisms and paths.

3.2 Study site

The investigated sewer system is located near the provincial city of Graz in the south-eastern parts of Austria. It can be categorized as a combined sewer network [2], thus transporting the daily wastewater flow of around 13000 persons as well as the runoff from eventual storm events. In recent years Austrian politics promoted the fusion of smaller wastewater systems, thereby subsequently increasing long intercepting sewers. Consistent to the program in 2004 two new power mains were installed in order to secure proper wastewater transport. Ever since, community complains of odor rose, caused by the degassing of H_2S and NH_3. Therefore, the manhole covers of populated areas were sealed, while the sewer sections of sparsely populated regions remained perforated. In order to prevent anaerobic conditions within the power mains, air is pumped into the storage basins. The new sewer system comprises a concrete storage basin, where the wastewater of the surroundings were collected and pumped through the first power main every six hours. The primary power main is constructed with cast iron and polyethylene (PE), with a bore of 200 mm and a length of 4

km. Thereafter a section of a PE gravity sewer, comprising around 50 concrete manholes and two small income pipes of residential areas, follows for another 5 km. Subsequently, the wastewater is collected within another storage basin from which it is continuously pumped into the second power main with a length of 3.5 km and 300 mm aperture. The final part of the system holds another gravity sewer section before concluding into a purification plant. C_3A free, B 400/WU/SA/TS7HS concrete was used following the guidelines of ÖN B 4200-10. Figure 4 displays a strong deteriorated manhole within the first gravity sewer section, while a schematic map of the sewer system is shown in Figure 5.

While the concrete of the storage basins show no sign of corrosion, the manholes of the gravity sewers are often strongly deteriorated. The upper few concrete layers reveal mushy rigidity and can be scratched down with bare hands. With flow distance the intensity of the corrosion decreases, resulting in non-corroded manholes at the end of the gravity sewer sections. The transported wastewater comprises mainly domestic wastewater, although one surface quarry and some minor commercial areas are also discharging into the system. Nevertheless, the quality and chemical composition of the wastewater lies within the standing orders for communal wastewater.

Figure 4: Strong deteriorated concrete in one of the manholes of the first gravity sewer section.

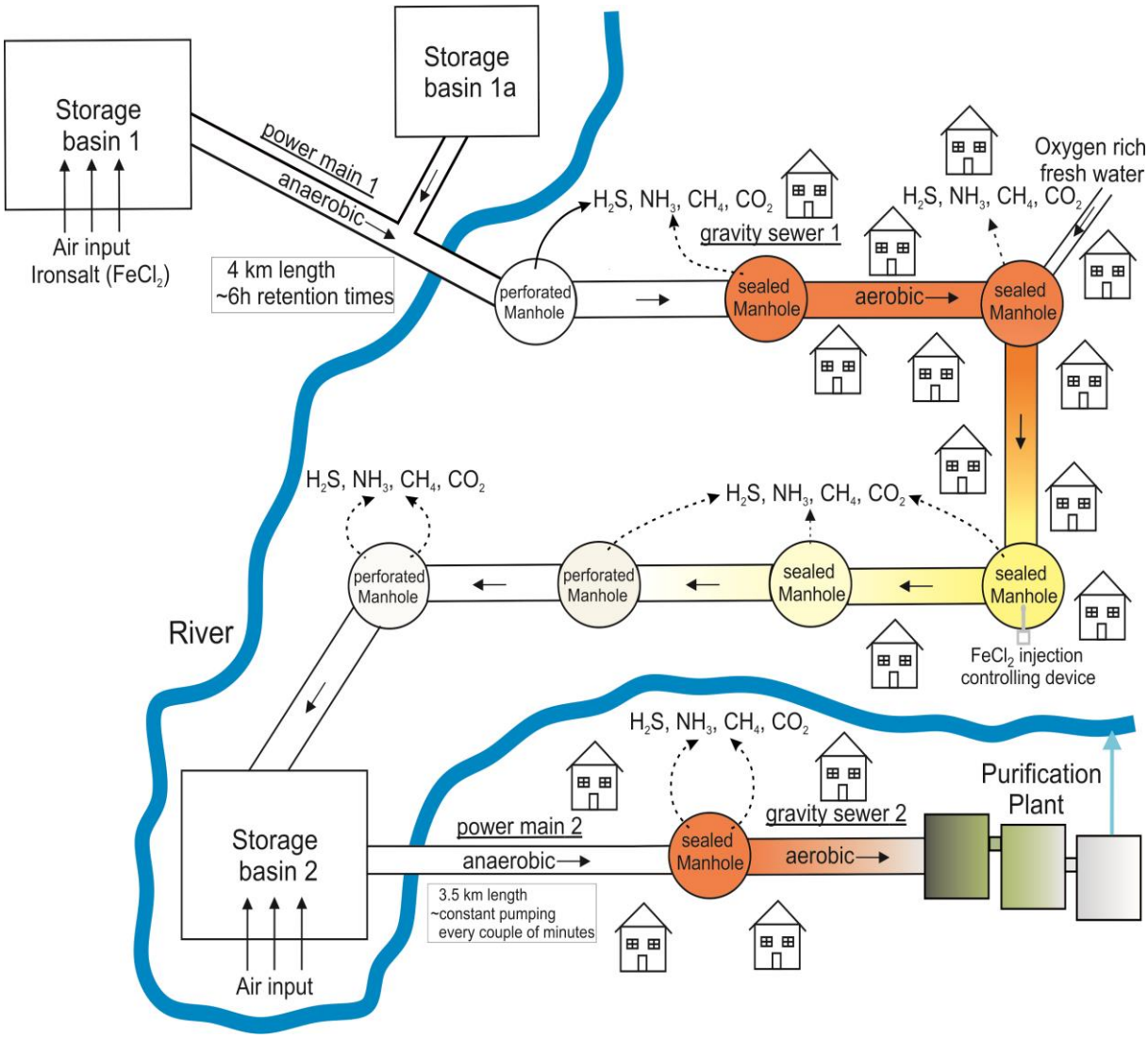

Figure 5: Schematic map of the sewer network. The intensity of the corrosion is indicated by red and yellow colours, red indicating areas of intense deterioration of the concrete. Noticeable is the concordance of the intensive corrosion and the sealed manhole covers. Intensive degassing of H_2S, CO_2 CH_4 and NH_3 is indicated with solid arrows within the upper parts of the system and the partly perforated manhole covers, while lower rates are indicated with doted arrows. The injection controlling device regulates the amount of iron-salt ($FeCl_2$) added to the system, depending on H_2S concentrations within the atmosphere of the selected manhole.

3.3 Methods and Materials

Solids and liquids from different manholes and the storage basins throughout the whole system were collected for analyses. Gas measurements were conducted within several manholes to value concentrations of H_2S, CO_2 and CH_4. Additionally, the results of previous studies, carried out by Ing. Mag. Rudolf Treffinger and engineering company Bilek & Krischner GmbH were taken into account.

3.3.1 Solids

Deteriorated concrete from different sites was sampled and shoveled into plastic bags. The samples were dried at 40°C, and subsequently grounded for chemical analysis using a PANalytical X'Pert PRO X-ray Powder Diffractometer (XRD) equipped with a Co-tube (45 kV and 40 mA), a rotating sample stage, a 0.5° divergence and antiscattering slit and an X'Celerator detector. Mineralogical phase identification was carried out with PANalytical X'Pert HighScore (version 2.2e). Thin sections of drill core samples were produced for back scattered images (BSE) and element mapping, using a JEOL JXA-8200 Superprobe (EMPA). Total carbon content was determined in dried samples and total organic carbon content was determined in dried and acidified samples as well as sulfur contend by combustion within a LECO C-230 Carbon Analyzer. Secondary electron images (SEI) of deteriorated concrete were mugged using AuPd sputtered samples in a Zeiss DSM 982 Gemini scanning electron microscope.

3.3.2 Liquids

Liquids were sampled throughout the whole sewers system for chemical analyses. Furthermore, samples of drinking water from the surrounding region were sampled in order to gain reference data. On site measurements of pH, electric conductivities, O_2 concentrations and redox potentials were carried out. In the lab the samples were centrifuged using a Avanti^{TM}-J-25I centrifuge in order to remove the coarse arrears and subsequently filtered

using 0.45 µm membranes for alkalinity analyses by potentiometric titration with 0.005 M HCl. The concentration of dissolved components was measured by a Dionex ICS-3000 Ion Chromatograph (IC) and PerkinElmer Optima 8300-TV inductively coupled plasma emission spectrometer (ICP-OES). Total organic carbon was analyzed using a Shimadzu TOC-VcPH+ASI-V Analyzer (TOC). Additionally, a hydraulic press was used to extract the pore fluids of the concrete for chemical analyses [28]. Between 800-11000 g of the deteriorated concrete was filled into a steel cylinder of a special adapted press and pressurized with a maximum of 1200 kN/mm^2. The squeezed pore solutions were sucked into a syringe and instant measurements of pH and conductivity were conducted. Subsequently, the samples were filtered with a 7 µm membrane followed by 0.45 µm membrane. In order to catch potential changes in pore fluid chemistry with increasing pressure, multiple samples were taken during one expression experiment. Afterwards, the solutions were analyzed according to the methods described above.

3.3.3 Gas Phase

Concentrations of gaseous H_2S, CH_4 and CO_2 within the sewer pipe atmosphere were measured, using a Draeger 3000 gas monitor. Three years ago VTA Technology GmbH established long term gas observations in order to monitor the impact of iron chlorine ($FeCl_2$) on gaseous H_2S emission. These data were evaluated. Furthermore, measurements during several surges, when emptying the power mains were conducted.

3.3.4 Bacteria Analyses

Concrete samples were taken in order to extract and identify occurrent bacteria. One gram of each sample was crushed and spiked with a 0.9% NaCl solution, before inoculated into a Thiobacillus Broth for incubation at 25-30 °C for 7 days. The Thiobacillus broth was composed after the Thiobacillus Agar 788, containing mainly thiosulfate (S_2O_3) and diverse salts [29, 30]. Grown bacteria were extracted and but in a hydraulic medium for selective incubation, consisting of the Thiobacillus Agar 788 and plus 0.2 g precipitated sulfur powder. The emerged bacteria were analyzed with 16S rRNA gene-based molecular techniques. Results were justified with the 16S rRNA database by Eurofinz MWG Operon.

3.3.5 Stable Sulfur Isotopes

Stable sulfur isotope ratios ($^{34}S/^{32}S$) were analyzed by combustion of $BaSO_4$- or ZnS- using a Thermo Finnigan 253 mass spectrometer [31]. The $\delta^{34}S$ values, gained from $BaSO_4$ represent samples extracted from the wastewater and concrete throughout the whole system. The $\delta^{34}S$ values obtained from ZnS reflect the signature of gaseous hydrogen sulfide (H_2S), which was captured by a 5% Zinc Acetate solution and consequently precipitated as ZnS. Results are given in $\delta^{34}S$-notations in ‰ relative to the Vienna-Canyon Diablo Troilite (V-CDT) standard.

3.4 Results

3.4.1 Deteriorated Concrete

XRD results taken from drilling cores represented unaltered concrete containing quartz, muscovite, albite and anorthite. Samples, extracted from the mushy, strongly deteriorated concrete consisted mainly of gypsum (30-63 wt. %) with certain amounts of quartz, anorthite or albite representing the residuals of the aggregates. In some corroded samples the sulfate salt bassanite ($CaSO_4 \cdot 0.5H_2O$) was found, indicating extremely high concentrated pore fluids at possible thermodynamic disequilibrium conditions. Typical XRD pattern are shown in Figure 6. The amount of total carbon ranged between 0.17 and 0.78 wt. % throughout the whole system, with TOC values from 0.12 to 0.51 wt. % (given in respect to C) and TIC values, when present, between 0.02 and 0.26 wt. %. Complete chemical data of all concrete samples can be seen in the appendix A1.

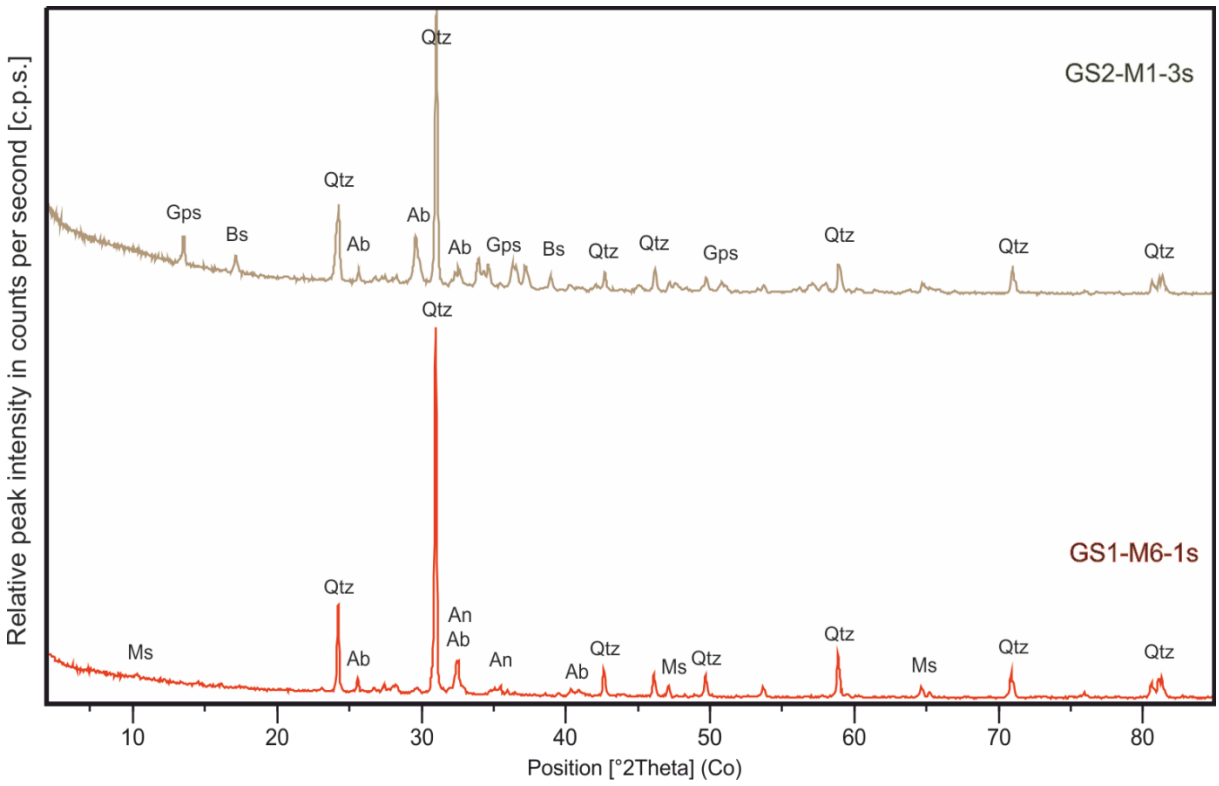

Figure 6: The GS1-M6-1s XRD pattern represents the unaltered concrete, containing quartz (Qtz), anorthite (An), albite (Ab), and muscovite/illite (Ms. The upper pattern (GS2-M1-3s) shows strongly deteriorated concrete, consisting of mainly gypsum (Gps) and bassanite (Bs) and residuals of quartz and albite.

Microprobe analyses clearly display proceeding transformation of the cementitious matrix into gypsum. Residuals of the aggregates, mainly quartz, feldspar (albite and anorthite) and mica (muscovite/illite), as well as distinct iron oxides and ilmenite ($TiFeO_3$) remain unaltered. Carbonate phases were gradually dissolved and transformed into gypsum. Clear separation between highly altered cementitious matrix displaying massive formations of gypsum and minor or unaltered concrete can be drawn. The processes and observations described in this chapter can be followed from Figure 7 and Figure 8.

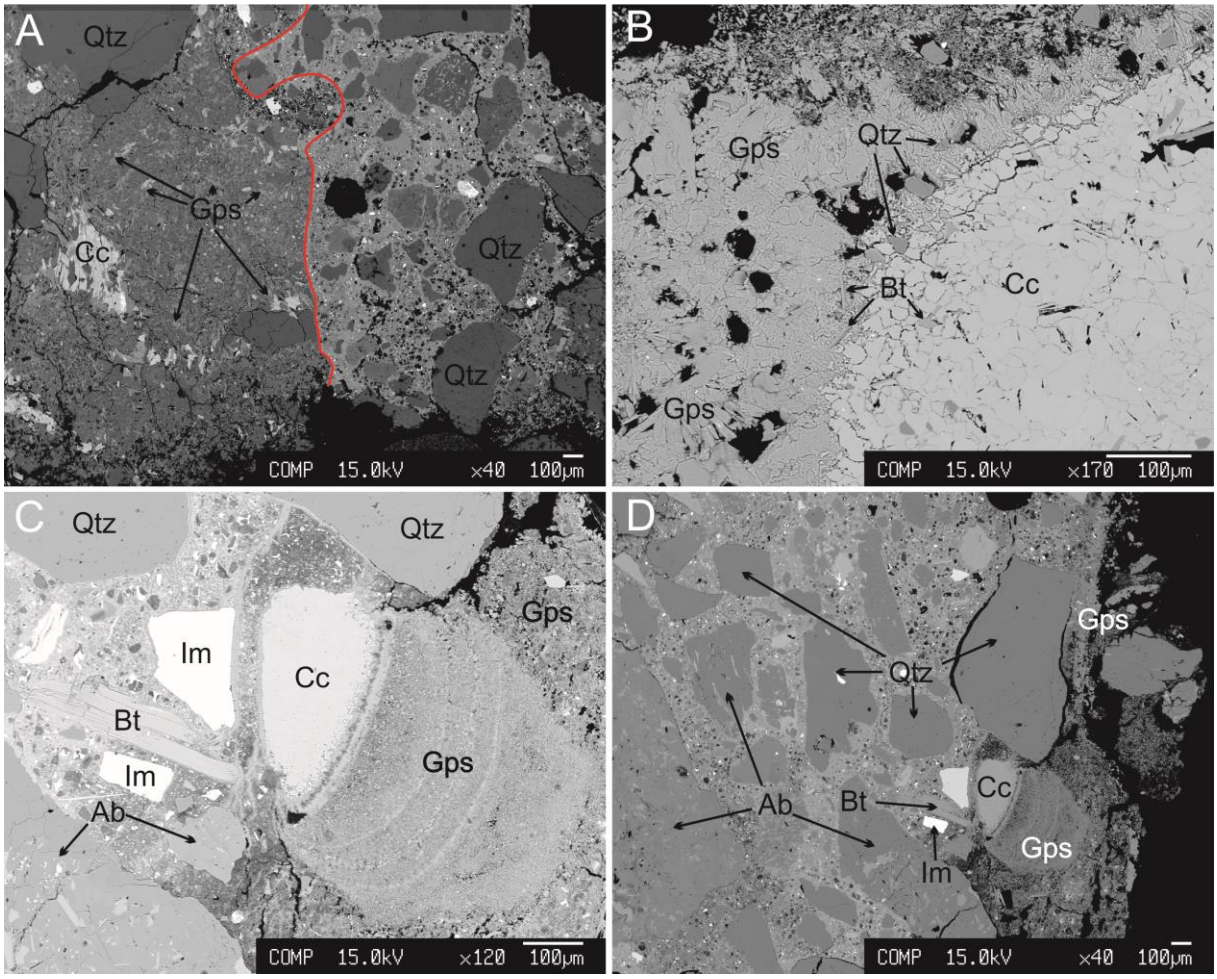

Figure 7: Displays partly altered concrete. Top left (A) shows the sharp front between strongly deteriorated concrete with massive gypsum (Gps) formation on the left side and low altered concrete on the right side. Top right (B) displays the gradual transformation of a calcite (Cc) into gypsum. Bottom right (C) shows a propagating corrosion front advancing from the right side, causing dissolution of calcite and formation of gypsum. Bottom left (D) displays an enlarged view on the partly transformed calcite grain.

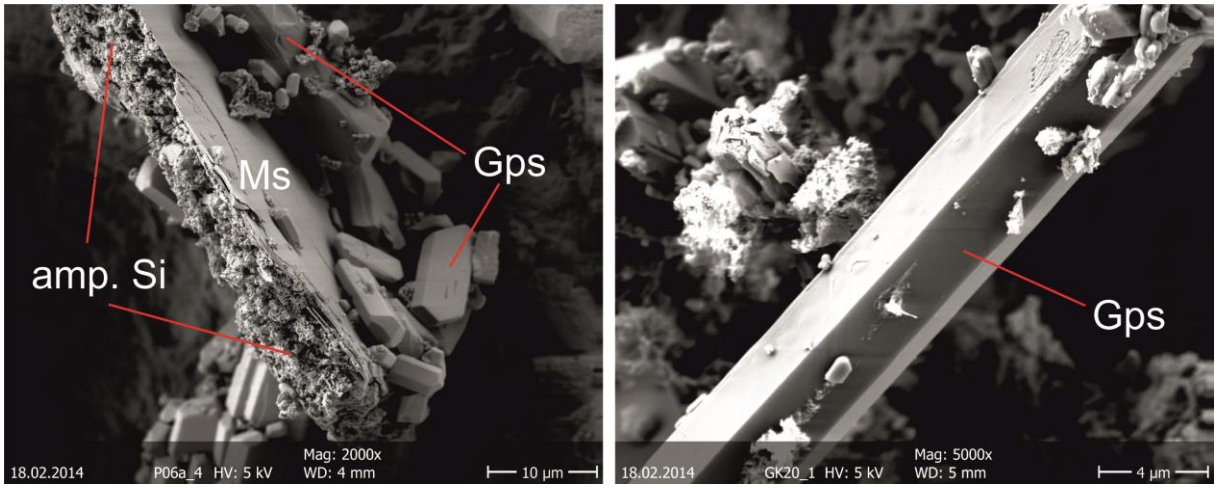

Figure 8: SE pictures, showing gypsum (Gps) crystals which formed during the corrosion process as well as mica [11] crystals and amorphous silica (amp. Si).

3.4.2 Solution Chemistry

Three types of different solutions were chemically analysed. Total chemical compositions are listed in the appendix A2. The first type comprises compositions of wastewater samples taken throughout the whole system. A clear decrease in pH from 8.0 ± 0.2 within the storage basins (SB1 and SB2) down to 7.4 ± 0.3 within the sections of the gravity sewer (GS1 and GS2) occurred. Consistently, intensive changes within the redox potential from values between +51 to -69 mV within SB1 and +32 mV in SB2, down to -248 mV within GS1 and as far as -320 mV in GS2 were measured. Occurring re-oxidation could be quantified within GS1, where O_2 concentrations increased from 1.4 mg l^{-1} in the first manhole up to 4.3 mg l^{-1} within SB2. Interestingly, O_2 concentrations at SB1 were extremely low between 0.2 and 0.8 mg l^{-1}. In SB1 sulfate concentrations from 64 to 115 mg l^{-1} SO_4^{2-} were measured, which decreased down to 25 ± 15 mg l^{-1} SO_4^{2-} in the first manholes of GS1 after the upper power main (PM1) of the system. With flow direction continues increase in SO_4^{2-} concentrations occurred. Finally, in SB2 up to 249 mg l^{-1} SO_4^{2-} could be quantified. After the second power main (PM2), again low SO_4^{2-} concentrations of 30 ± 15 mg l^{-1} occurred. Representative values of wastewater chemistry are displayed in Table 2. Additionally, Ca^{2+} concentrations between 27 and 148 mg l^{-1}, Mg^{2+} concentrations of 10 ± 5 mg l^{-1}, K^+ concentrations of 21 ± 12 mg l^{-1}, Na^+ concentrations between 37 and 138 mg l^{-1} and CL^- concentrations from 25 to 214 mg l^{-1} could be quantified.

Table 2: Typical values of wastewater chemistry along the flow distance (all analyses are displayed in appendix A2). Samples were extracted from the two storage basins (SB1-5aq and SB2-2aq) as well as from the first (GS1-M1-1aq), 6th (GS1-M3-6aq) and 8th (GS1-M4-2aq) manhole of gravity sewer 1, as well as from the first manhole of gravity sewer 2 (GS2-M1-6aq).

Sample ID	pH	T °C	Conductivity µS/cm	Redox mV	O_2 mg/l	SO_4^{2-} mg/l	Ca^{2+} mg/l	NO_3^- mg/l	DOC mg/l
SB1-5aq	8.18	10.0	1744	51	3.15	74	65	2.63	73
GS1-M1-1aq	7.39	8.0	1705	-157	1.38	41	74	bdl.	64
GS1-M3-6aq	7.424	17.7	1394	-209	1.63	23	66	bdl.	56
GS1-M4-2aq	7.25	9.1	1509	-248	1.80	152	114	bdl.	83
SB2-2aq	7.80	9.6	1771	32	4.26	249	147	bdl.	83
GS2-M1-6aq	7.65	13.5	893	-320	0.52	28	49	bdl.	28

The second type consists of the interstitial fluids, extracted from the deteriorated concrete. These fluids showed extreme low pH values between 0.7 and 2.6. At the same time they displayed extreme high concentrations of SO_4^{2-} between 2 and as high as 102 g l^{-1}. Additionally, high concentrations of Ca^{2+} (550 ± 100 mg l^{-1}) and Mg^{2+} (52 to 4321 mg l^{-1}) and NH_4 (63 to 2994 mg l^{-1}) were measured. In general a strong correlation between pH and concentration of dissolved ions could be drawn, displaying increasing concentrations with rising acidity. Interestingly, Ca does not follow that trend, but displayed quite constant concentrations. Typical enrichment trends can be seen in Table 3. The third type of analysed liquids comprises samples of the local drinking waters (TW), taken from all 3 communities concerned which showed SO_4^{2-} concentrations of 34 ± 16 mg l^{-1}. All concentrations of the major dissolved ions within the interstitial solutions are displayed within the appendix A3.

Table 3: Displaying interstitial fluids from strongly deteriorated concrete of GS1 (GS1-M2-PF1, GS1-M3-PF2 and GS1-M3-PF4) and GS2 (GS2-M1-PF1 and GS2-M1-PF3).

Sample ID	pH	T °C	Conductivity µS/cm	SO_4^{2-} mg/l	Ca^{2+} mg/l	Mg^{2+} mg/l	NH_4^+ mg/l	NO_3^- mg/l
GS1-M2-PF1	2.42	21.3	5650	2719	577	52	81	9
GS1-M3-PF2	1.60	22.4	20400	9951	621	206	315	45
GS1-M3-PF4	1.58	21.8	18280	7750	494	126	370	29
GS2-M1-PF1	0.83	21.4	102000	104210	551	4322	2994	7
GS2-M1-PF3	0.71	22.2	100900	40818	567	990	210	5

3.4.3 Distribution of stable sulfur isotope

The results of the sulfur isotope measurements are displayed in Figure 14. The samples, precipitated as $BaSO_4$ from wastewater showed $\delta^{34}S$ values of the dissolved sulfate ranging around 6 ± 3 ‰ (VCDT). With flow distance, enrichment in heavy versus light S isotopes could be detected. Signals of interstitial fluids, extracted from the pore volume of the deteriorated concrete displayed significant lighter signatures from -2 ± 2 ‰. Accordingly, $\delta^{34}S$ values measured within the corroded concrete showed values of -2 ± 2 ‰ as well. Interestingly, isotopic signatures, derived from ZnS, which refers to the gaseous H_2S, comprised $\delta^{34}S$ values similar to the $\delta^{34}S$ values caught within the wastewater between 7 and 8 ‰.

3.4.4 Bacterial analyses

Bacteria, extracted from deteriorated concrete samples were identified by 16S rRNA sequencing as Acidithiobacillus Thiooxidans and Acidithiobacillus Ferrooxidans. The measured pH within the petri dish used for bacteria growth, dropped within the first week below 2. The reconciliation with the 16S rRNA database showed conformities of >99%.

3.4.5 Gas measurements

Data of long term gas measurements provided by VTA Technology GmbH, showed average concentration of 1.3 ppm H_2S and a large variation between below the detection threshold and 124 ppm within the 8th manhole of GS1during active $FeCl_2$ addition. Due to maintenance work conducted between 2.12.13 and 9.12.13 no $FeCl_2$ was added to the system. Contemporaneously, H_2S values of above 440 ppm were measured. Typical H_2S long term concentration variations can be seen in Figure 9. Gas measurements conducted during sampling displayed concentrations up to 84 ppm H_2S within the first 8 manholes of the gravity sewer sections. With flow direction continues decrease in gaseous H_2S concentrations was detected, resulting in manholes with no occurring emission. In contrast, constantly high CO_2 concentrations of up to 0.26 vol. % throughout the whole system were measured with no decreasing concentration trend or what so ever. Additionally, methane (CH_4) concentrations of up to 4 vol. % were measured within the first 6 manholes of the GS1 and within the first of GS2.

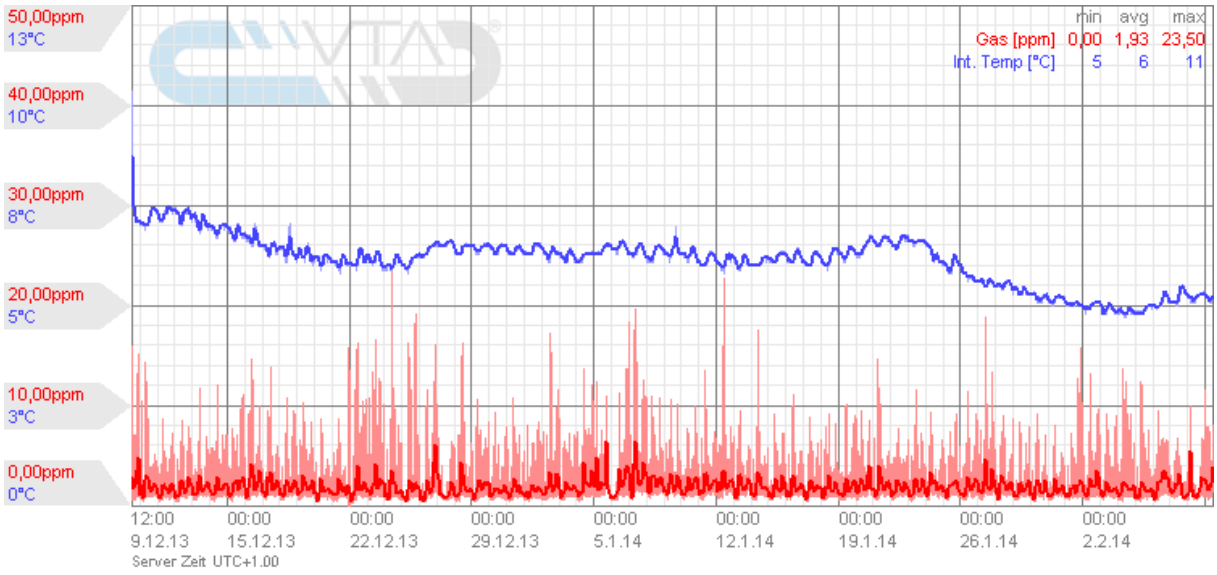

Figure 9: Typical evolution of H_2S concentrations within the 8th manhole of the system measured by VTA Technology GmbH.

3.5 Discussion

The results given clearly proved that the occurring concrete corrosion can be attributed to microbial induced concrete corrosion (MICC). Measured redox potentials down to -320 mV as well as low oxygen levels clearly indicated prevailing anaerobic conditions and bacterial activity within the power mains. There, anaerobic autotrophic organisms, mainly of the genus Desulfovibrus and Desulfobulbus oxidized organic matters, using sulfate as electron acceptor in the absence of oxygen and nitrate [20]. This process resulted in the formation of sulfide species, including its gaseous form of H_2S due to prevailing pH values between 7 and 8. The sulfide production could also be verified due to significant decrease in sulfate concentrations throughout the flow direction of the power mains, from an average of 105 to as low as 14 mg L^{-1}. The H_2S was liberated from the wastewater into the manholes atmospheres, where concentrations of up 400 ppm could be measured. Additionally, concentrations of CO_2 up to 0.26 vol. % and CH_4 up to 4 vol. % were quantified. CH_4 is a byproduct of methanogenesis, which typically proceeds under redox potentials below 200 mV [2]. It is reported to occur in areas of the power main where sulfate depletion is present [32]. The schematic view of the main anaerobic microbial processes is exemplified in Figure 10.

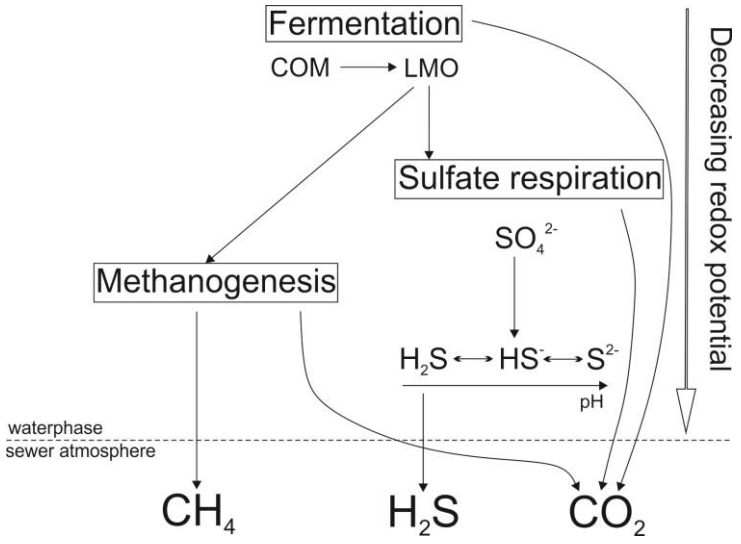

Figure 10: Schematic view of the 3 microbial processes occurring under anaerobic conditions [2]. Initial transformation from complex organic molecules (COM) into low molecular organics (LMO) through a series of reduction and oxidation processes. LMO are consumed by sulfate reducing bacteria as well as methane-producing bacteria resulting in sulphides, methane (CH_4) and CO_2 production. Notice that the single processes start at distinct redox potentials.

The liberation of volatile components from the water phase was controlled by change in surrounding partial gas pressure, temperature and flow turbulences [33]. The latter seemed to engage in a central role during the degassing sequence of the volatile components. After the second power main the water entered the gravity sewer section two meters above the channel bottom, creating a waterfall. Interestingly, increased decline in gaseous concentrations with flow direction could be measured. Simultaneously, increased corrosion intensity could be seen within this first manhole, and finally no further deterioration could be detected within adjacent manholes.

After entering the sewer atmosphere H_2S got absorbed into the outer layers of the concrete walls, where it oxidized over a chain of complex reaction paths [7, 33, 34], with sulfuric acid (H_2SO_4) as the final product. There is evidence to suggest that diffusion of gaseous H_2S into the concrete increased significantly within manholes with sealed covers, since no ventilation out of the manhole atmosphere could occur, creating an environment similar to a bioreactor. In consequence, strongly deteriorated manholes matched those with sealed covers. However, it is not completely verified how sealed covers attribute to intensifying the corrosion, since all those strongly deteriorated manholes were situated within the first part of the gravity sewers, where intensive degassing occurred. During the early stages of the MICC attack abiotic H_2SO_4 production occurred due acid-base reactions between the H_2S and pore fluids of the

concrete. Additionally, carbonation due to the interaction between CO_2 and the calcium hydrate phases of the cementitious matrix took place. Both processes altered the pH from initially around 12.5 down to around 9.5. Starting from there progressive colonization of aerobic heterotrophic bacteria took place and biotic H_2SO_4 production proceeded. With constantly decreasing pH different strains of sulfur-oxidizing bacteria colonized the pore volume. Figure 11 displays the distribution of neutrophil bacteria i.e. Thiobacillus Tioparus, and acidophil bacteria of the genus Acidithiobacillus with pH. The identified bacteria Acidithiobacillus Thiooxidans and Acidithiobacillus Ferrooxidans thrive until pH <1, if sulfate concentrations exceed 74 g l^{-1} [24], which could be verified due to measured concentrations up to 102 g l^{-1}.

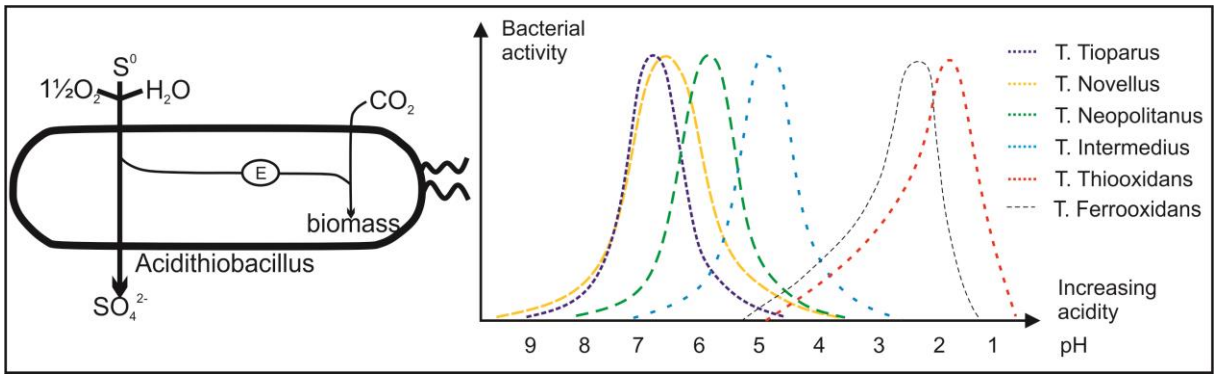

Figure 11: Top right shows the activity of different strains of bacteria with pH. Top left displays a schematic view of sulfur-oxidizing bacteria. I.e. elemental sulfur (S^0) is used as energy source, thereby oxidized to sulfate (SO_4^{2-}). Carbon from CO_2 is used as biomass [14].

The H_2SO_4 produced triggered dissolution of the cementitious matrix and secondary formed carbonates as well as massive formation of gypsum. XRD analyses clearly indicated that within the heavily corroded concrete complete dissolution of the pristine cementitious matrix occurred, linked with gypsum formation up to 63 wt. %. Expected ettringite formation lacked due to its high solubility at pH values present. Microprobe analyses displayed gradual depletion of the C-S-H phases within the cementitious matrix and adherent partly dissolution due to propagating corrosion. During the course of this transformation subsequent integration of sulfur into the concrete matrix proceeded, with coinstantaneous depletion of silica, calcium and magnesium occurring. In general, the integration of sulfur proceeded along cracks and grain boundaries of the additives, before propagating throughout the whole matrix. The dissolved ions, i.e. Mg^{2+}, Ca^{2+}, Na^{+}, or NO_3^{-} were continuously enriched within the interstitial solutions resulting in high concentrations of total dissolved solids (TDS). Most relevant element distributions are displayed in Figure 12.

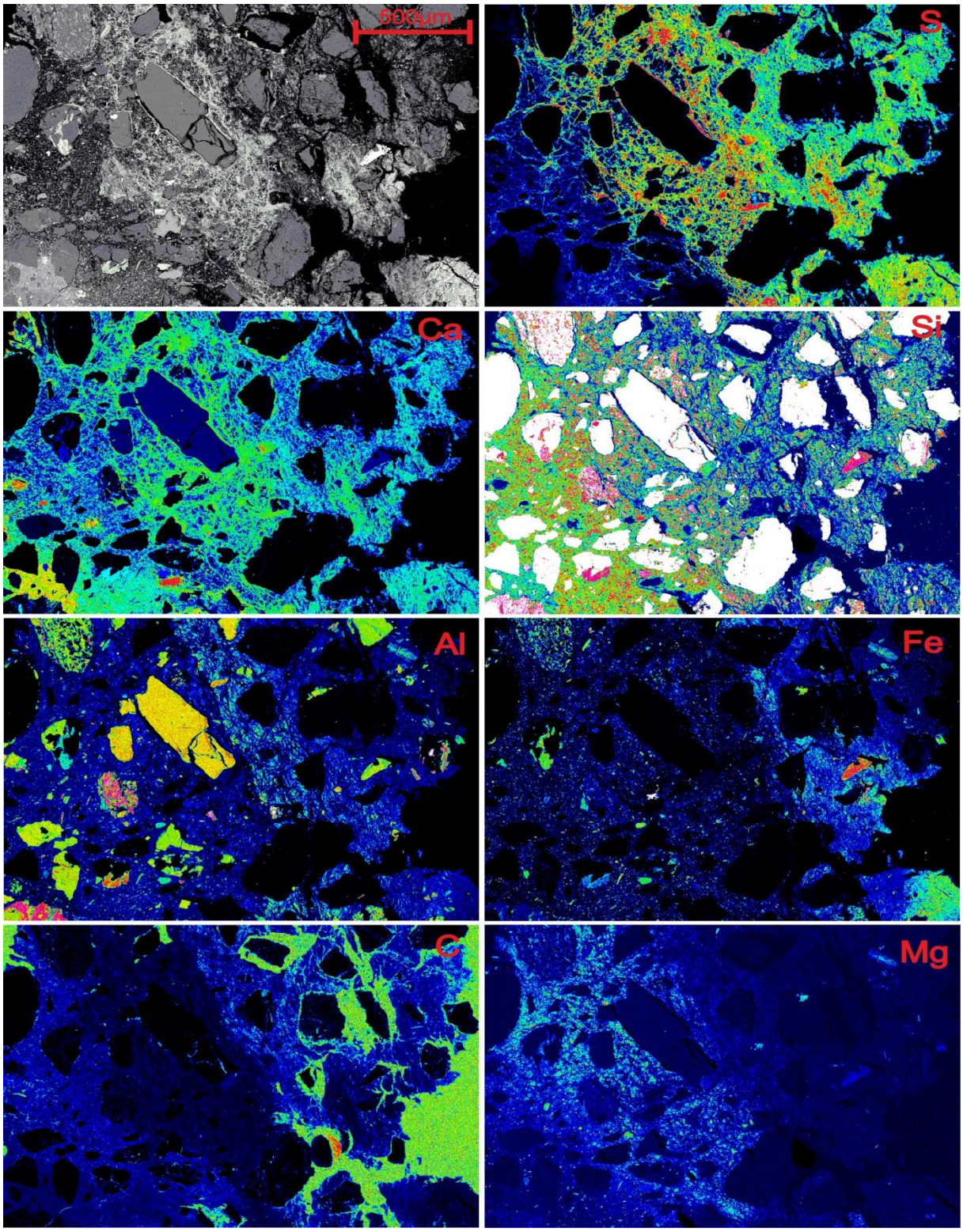

Figure 12: Shows elemental mapping of sulfur (S), calcium (Ca), silica (Si), aluminium (Al), iron (Fe), carbon (C) and magnesium (Mg). The propagating corrosion front emanates from top right to bottom left. Notice the opposing trend of Si and S enrichment. Ca concentrations decrease with increasing S concentrations due to dissolution of calcite and calcium hydrates, but gets partly incorporated within the newly formed gypsum crystals.

Element mapping of the transition zones between unaltered and strongly deteriorated concrete revealed areas where Mg, Al and Fe enrichment is visible. This can be explained with pH

depending stability of single Mg, Al and Fe bearing phases. Mg containing phases within the cementitious paste i.e. brucite ($Mg(OH)_2$) were stable until a pH of around 10. If the pH declined below that level, dissolution occurred. Due to its amphoteric characteristics, Al accumulated as aluminium hydroxide ($Al(OH)_3$) in areas where the pH ranged between 10 and around 4 [35]. The explanation for Fe accumulations within areas with pH <4 could be given by the first appearance of Acidithiobacillus Ferrooxidans under these conditions. Acidithiobacillus F. have the ability to oxidize Fe (II) to Fe(III), which possesses significant lower solubility and precipitated in the form of diverse iron oxides. Modelling of the pore fluids carried out sowed minor gypsum oversaturation (SI_{Gps} = 0.07 ± 0.1) and undersaturation in matters of brucite (SI_{Bc} = -16 ± 2) and bassanite (SI_{Bs} = -0.8 ± 0.1). Summarizing it could be concluded that within the transition zones between strongly deteriorated and unaltered concrete sequences of mineral dissolution and re-precipitation occurred, which were controlled by pH changes. Accumulation zones of Mg, Al and Fe are displayed in Figure 13.

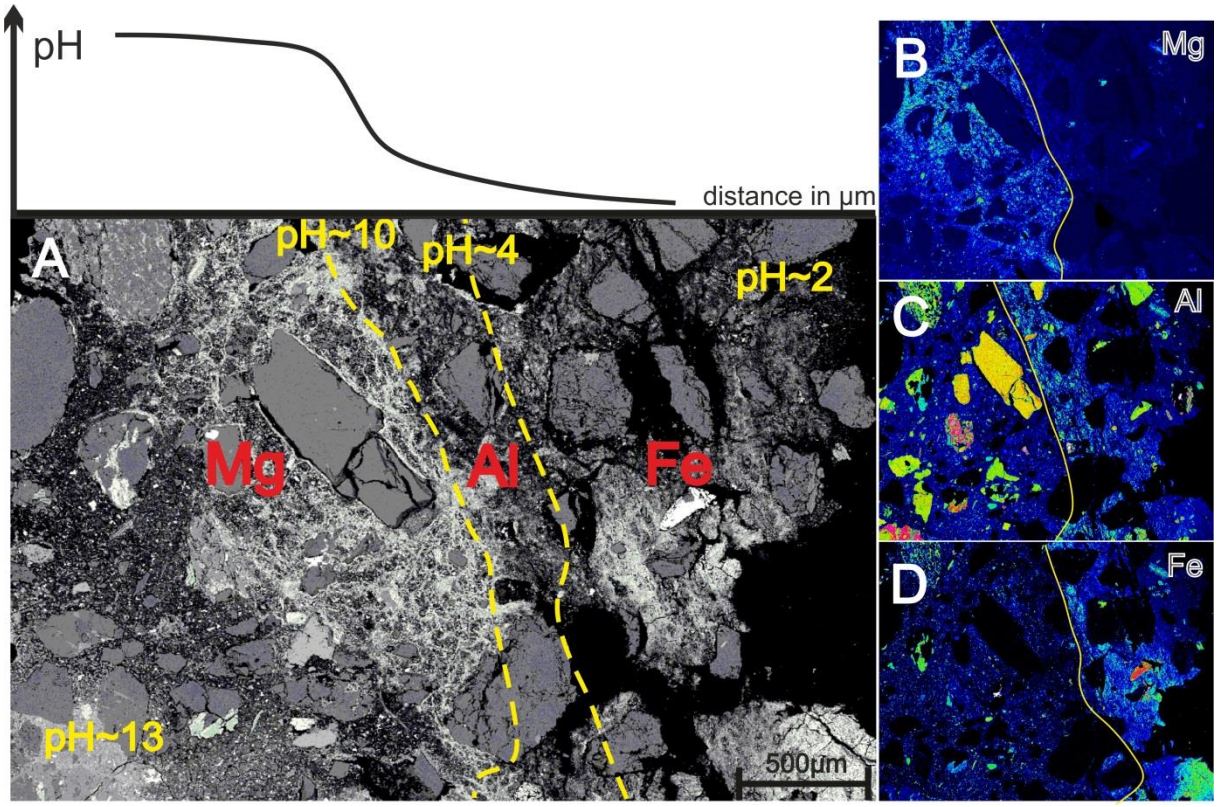

Figure 13: Displaying the pH depending dissolution and re-precipitation of Mg, Al, and Fe within a progressive corrosion front from the right to the left side (A). Mg accumulations indicate pH >10 (B) while Al is enriched in areas with pH between 4 and 10 (C). Fe enrichment can be explained by the ability of Acidithiobacillus Ferrooxidans to oxidize Fe (II) to Fe (III). Fe (III) shows significant lower solubility than Fe (II) and therefore precipitates as diverse iron oxides until pH~2 (D).

Measurements of stable sulfur isotopes clearly support bacterial activity. An isotope fractionation is obvious between samples extracted from the water phase and the newly formed gypsum. This clearly supports bacterial activity as the thriving force behind the sulfur cycle of the system. The comparatively small isotopic fractionation of 6-10 ‰ (VCDT) could be explained by almost quantitative transformation of the occurring SO_4^{2-} concentrations within great parts of the power main. Supporting evidence were low SO_4^{2-}concentrations within the upper parts of the gravity sewer. Also the production of CH_4 indicated almost complete depletion of sulfate within the power main, since methanogenesis only occurs in areas where no or low sulfate concentrations are present [32]. Interestingly, no isotope fractionation of ^{34}S versus ^{32}S could be seen between gaseous H_2S (extracted via ZnS precipitation) and the dissolved SO_4^{2-} of the wastewater. Further research has to be carried out before a more detailed interpretation concerning the latter issue can be developed. However, isotope fractionation between H_2S and SO_4^{2-} throughout bacterial activity support the assumption of quantitative transformation of the SO_4^{2-} concentrations present within the power mains, as non-quantitative transformation would result in large kinetically controlled fractionation effects. Isotopic fractionation is displayed in Figure 14.

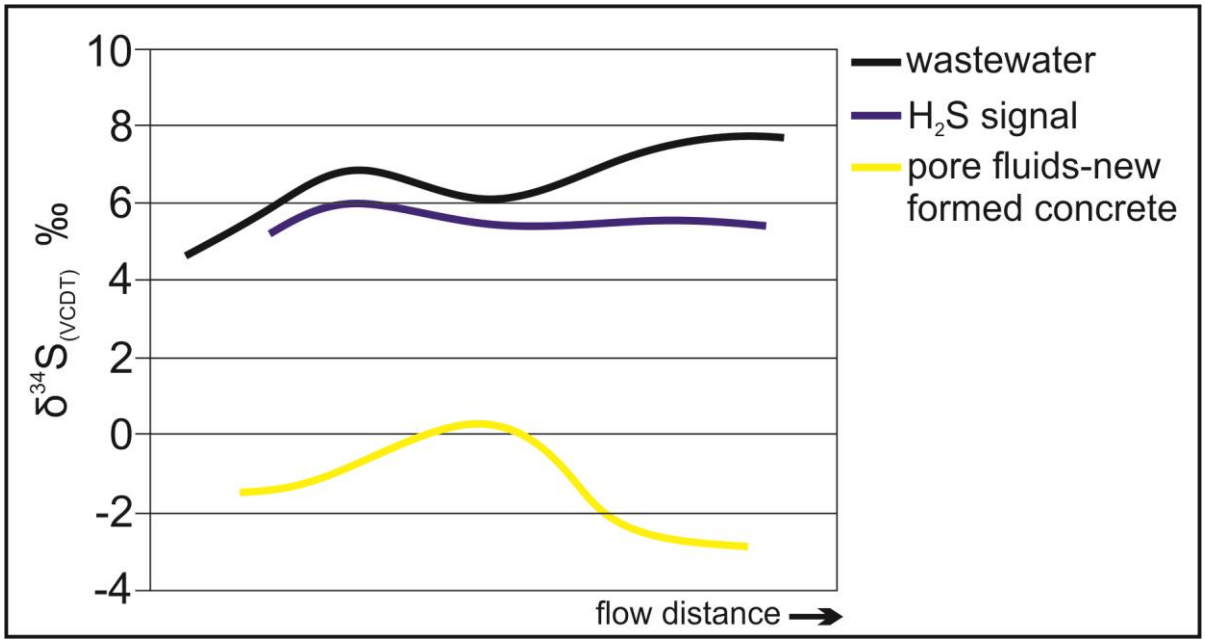

Figure 14: Measured $^{34}S/^{32}S$ isotope fractionation displayed as $\delta^{34}S$ values according to VCDT, between the dissolved SO_4^{2-} in the wastewater, the gaseous H_2S, the SO_4^{2-} in the pore fluids and the secondary formed gypsum in the deteriorated concrete with flow distance.

4 Corrosion mitigation methods

In general there are two possible approaches to avoid the concrete corrosion present, thus a sustainable remediation can be conducted. The first method of resolution comprises the inhibition of H_2S formation within the system, while the second approach targets the control management of the sulfide species present. This chapter aims to describe and discuss various solutions which are applied worldwide plus ideas fitted to the distinct system characteristics present. Additionally, the application of calcium aluminate cement (CAC) as possible high chemical resistant material within these aggressive environments is discussed.

4.1 Inhibition methods for H_2S formation

Anaerobic conditions are central for sulfate reduction since prevailing bacteria favor nitrate and oxygen prior to sulfate as electron acceptors. One possible solution is thus the prevention of anaerobic conditions due to the increase of the redox potential through addition of alternative electron acceptors like nitrate or oxygen. Oxygen can be added as air or pure oxygen, although it must be reconsidered when injecting air that only around 20 % of its volume consist of oxygen and great amounts of inert N_2 gas, which may accumulate somewhere in the system. [2] Injecting pure oxygen resolves this problem although it has to be taken into account that its technical utilization is more complex than with air and storage tanks have to be kept at the injection point. Addition of nitrate will produce anoxic conditions and can be added in the form of various salts e.g. $Ca(NO_3)_2$. Its purpose is to diminish the reduction of sulfates as well as reducing the bacterial activity within the system [36]. The addition of nitrate is much more expensive than oxygen and has to be regulated in order to avoid nitrate inflow into the purification plant located downstream.

Alternatively, increasing the flow rates due to injection of external water would reduce the existing biofilms and sedimentary deposits within the power mains. Abrasive shear forces along the sewer walls would be increased while deposits would be diminished. Additionally, external, oxygen rich water would delay the establishment of anaerobic conditions within the power main, thereby reducing the production rate of sulfide species.

Furthermore, mechanical cleaning of the sewer channels by using a cleaning pig can remove great parts of the biofilm and sedimentations along the sewer walls [16]. The channels have to

be cleaned routinely in order to prevent re-establishment of the biofilm. Also the geometry of sewer channels has to be taken into account. In general cleaning pigs are used together with other prevention methods.

4.2 Reduction and control management of existing sulfide species

This approach aims to control and obviate the damaging effects caused by degassing of H_2S. It is important to note that due to the following control managements no alteration within the prevailing anaerobic and strongly reducing conditions of the system are achieved.

There are several metal salts which can be used for sulfide precipitation within wastewater systems, with ferrous iron, Fe(II), and ferric iron, Fe(III), bond within iron-chlorines or iron-sulfates being the most common ones. Thereby, iron sulfide (exemplarily amorphous FeS is used in the following instead of pyrite, FeS_2) is formed according to the stoichiometry of the following equations [2]:

$$Fe^{2+} + HS^- \rightarrow FeS + H^+ \qquad \textbf{Equation 9}$$

$$Fe^{3+} + HS^- \rightarrow 2Fe^{2+} + S^0 + H^+ \qquad \textbf{Equation 10}$$

FeS is metastable under anaerobic conditions, but re-oxidizes when aerobic conditions might be re-established along the flow direction. Although Fe (III) works more efficiently, its reaction time is much slower. Therefore, the retention times of the wastewater have to be taken in account when choosing the proper additive. In general a mixture of ferric and ferrous solutions is reported to work the most efficiently. In order to achieve efficient sulfide precipitation by addition of iron, pH values ≤ 8 are central. In this matter it is important to consider that constant precipitation of FeS is continuously lowering the pH of the system. Therefore, alkaline substances like calcium hydroxide ($Ca(OH)_2$) or sodium hydroxide (NaOH) can be added to increase the pH level. [2]

Alternatively, chlorine (Cl_2) can be added to the wastewater, either directly in its gaseous form or as hypochlorite (OCl^-) or sodium hypochlorite (NaOCl). These chlorine species are oxidizing sulfide to elemental sulfur (S^0) or sulfate, following the reaction [2]:

$$HS^- + Cl_2 + OH^- \rightarrow 2Cl^- + S^0 + H_2O \qquad \textbf{Equation 11}$$

Caution is needed when working with OCl^- since it is extremely toxic for human beings. Furthermore, Cl_2 might inhibit the biological processes occurring voluntarily within the purification plant if the apportioning is wrong. One of the major advantages of chlorine addition is that it works efficiently at pH 7 to 8, conditions present in most communal wastewaters.

Another possible additive is hydrogen peroxide (H_2O_2) which oxidizes sulfides into S^0 or SO_4^{2-}. Additionally, it can partly degrade sulfate-reducing bacteria within the biofilm. On the downside it is quite expensive and therefore only used in certain cases. [2]

4.3 Calcium Aluminate Cement (CAC)

Remediation strategies incorporating calcium aluminate cements (CAC) are known to enhance the durability of concrete structures significantly compared to ordinary Portland cement (OPC) [37-39]. This is due to the fact that abiotic H_2S oxidation during the early stage of the MICC is less favorable within CAC mortars [39]. Furthermore, the higher acid neutralization capacity of $Al(OH)_3$ compared to Ca^{2+} decelerates the pH decrease, as shown in Equation 12 [38]:

$$Al(OH)_3 + 6H^+ \rightarrow 2Al^{3+} + 6H_2O \qquad \textbf{Equation 12}$$

Additionally, the hydrated alumina phases react with the H_2SO_4, creating an alumina gel layer which significantly decreases the porosity of the surface layers. The alumina gel layer forms promptly, resulting in significant lower H_2S diffusion rates, as well as lower oxygen penetration depths and limiting biofilm adhesion. Furthermore, AlH_3 is toxic for the neutrophil bacteria, creating bacteriostatic effects. CAC cement is best used with dolomitic aggregates (DOL), since this mortar combines the toxic effects of alumina together with porosity decrease and DOL alkalinity [39]. Since CAC/DOL mortars are significantly more expensive than OPC, they are often used as linings on concrete, made of cheaper compounds.

4.4 Resolution methods applied for this system

When contemplating the complex system characteristics of the sewer system present, not many realistic prevention methods can be applied. Due to a tight budget addition of more expensive but also more efficient additives like hydrogen peroxide or nitrate have to be ruled

out. The same accounts for the injection of external water, since the communities pay the purification plant operators per incoming liter. Due to the complex geometry and length of 4 km mechanical cleaning pigs could not be used efficiently. Therefore, a combination of ferrous and ferric iron salts together with alkaline compounds like calcium hydroxide seems to be the most reasonable solution. For this approach it is crucial to keep the pH $\geq$ 8 in order guarantee efficient FeS precipitation and to minimize the general $H_2S_{(g)}$ production as discussed in section 2.1.2. Since three years, ferrous chlorite ($FeCl_2$) had been added to the system, operated by VTA Technology GmbH. Ever since a significant decrease in H_2S concentrations could be achieved. Optimizing these additives due to the addition of Fe (III) and $Ca(OH)_2$ could lower the sulfide production rate to a level, where no damage to the concrete would occur. Additionally, the deteriorated concrete has to be removed and the remains be cleaned, i.e. using a high-pressure cleaner. Accordingly, CAC/DOL linings have to be applied in order to secure sustainability.

5 Conclusion and Outlook

Summarizing it can be stated that the application of a multi proxy approach is a very useful tool when investigating the complex reaction mechanisms of concrete corrosion. Affiliated chemical, biological, isotope and mineralogical analyses clearly linked the occurring corrosion to microbial induced concrete corrosion. The extreme aggressive interstitial fluids, caused by intensive colonization of sulfur oxidizing bacteria and subsequent H_2SO_4 production enhanced a fast propagating corrosion which led to complete deterioration of the concrete within only 8 years. Additionally, the dissolution and re-precipitation of distinct mineral phases within the propagating corrosion front could be linked to pH changes within this micro environment.

The elaboration of promising strategies in order to secure sustainable remediation is a central part within the further planned investigations. General approaches are discussed in chapter 4, although it must be stated that further research is necessary for reliable strategies. Optimizing the type of additive applied at the moment by addition of alkaline compounds or ferric iron has to be tested in order to determine the consequences reliably. From the scientific point of view further measurements of stable isotope signatures are planned, including sulfur, oxygen, hydrogen and carbon in order to gain better understanding of the occurring fractionation mechanisms and the related reaction paths for the individual sewer phases. Additionally, isotopic data can be used to determine the source of distinct elements i.e. sulfur, thereby identifying the possible input of industrial sites, located close to the system. Isochronal long term gas observation within different manholes along the flow direction are planned, thus the emission mechanisms of degassing volatile compounds can be analyzed. Finally, the development of a parameter based model for this sewer system should help to calculate the effects caused if single parameter would be changed. Ideally, the model developed within the present case can be applied on other sewer systems attacked by MICC.

6 Conference paper for the international conference of durability of building materials and components, in Brazil 2014.

BACTERIOGENICALLY INDUCED SULFURIC ACID ATTACK ON CONCRETE IN AN AUSTRIAN SEWER SYSTEM

Grengg, C. [(1)], Mittermayr, F. [(2)], Baldermann, A. [(1)], Böttcher, M. E. [(3)], Leis, A. [(4)], Koraimann, G. [(5)] & Dietzel, M. [(1)]

(1) Institute of Applied Geosciences, Graz University of Technology, Rechbauerstraße 12, 8010, Graz, Austria

(2) Institute of Technology and Testing of Building Materials, Graz University of Technology, Inffeldgasse 24, 8010, Graz, Austria

(3) Leibniz Institute for Baltic Sea Research (IOW), Seestraße 15, D-18119 Warnemünde, Germany

(4) RESOURCES – Institute for Water, Energy and Sustainability, Joanneum Research, Elisabethstraße 18/2, 8010, Graz, Austria

(5) Institute of Molecular Biosciences, Graz Karl-Franzens University, Humboldstraße 50, 8010, Graz, Austria

Abstract

The deterioration of the investigated Austrian sewage system is attributed to several complex processes, which are referred to as bacteriogenically induced sulfuric acid attack. Anaerobic bacteria, present within the sewage system had consumed the organic matter, thereby reducing sulfate to hydrogen sulfide (H_2S). Subsequently, degassing of H_2S followed by its oxidation by aerobic bacteria Acidithiobacilli within the concrete ultimately led to the formation of sulfuric acid. This sulfuric acid reacted with the cement paste to form gypsum and bassanite. These minerals finally caused the severe damage of the concrete in the manholes.

Various crucial parameters for detecting alteration features were determined in the field and laboratory, including (i) measurements of temperature, pH, alkalinity, chemical compositions of the solutions, (ii) characterization of the chemical and mineralogical composition of solids, and (iii), determination of gaseous H_2S, CH_4 and CO_2 concentrations within the sewer pipe atmosphere. Stable isotope data were used to decipher individual reaction mechanisms.

6.1 Introduction

Corrosion of concrete based sewer systems due to the emission of hydrogen sulfide from wastewater is a huge economical factor and worldwide occurring issue. The so-called biogenic sulfuric acid attack can reduce the lifespan of concrete structures dramatically, from expected 100 down to 30-50 years, in extreme cases even down to 10 years [1, 2]. The required remediation is challenging and demands high costs. For instance, the annual remediation charges of Los Angeles County exceeded €400 million in 1996 [3].

At the same time the reaction mechanisms and paths, which cause the deterioration of concrete are still under debate. In this study, we provide a deeper understanding about the driving forces of bacteriogenically induced concrete corrosion using a multi-proxy approach. For this purpose an Austrian sewer system which is urgently due for restoration, after a lifespan of only 8 years, was extensively investigated.

6.2 Site Description

The investigated sewer system is handling the wastewater of around 13 000 persons. In 2004, two power mains were installed, in order to achieve proper wastewater transport. Ever since community complains about odor rose and subsequently deterioration of the concrete within parts of the gravity sewer started. Figure 15 displays a schematic sketch of the sewer system and one of the heavily corroded manholes.

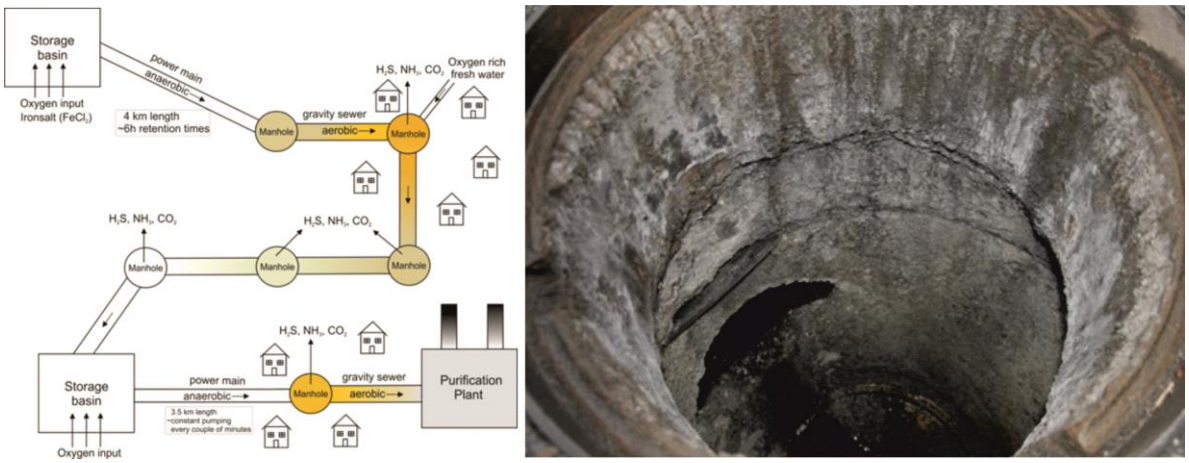

Figure 15: Left picture illustrates a schematic view of the sewer system with the two storage basins, the two power mains and the gravity sewer sections. Orange colours indicate intense corrosion, while grey colours represent low degradation degrees. On the right hand side one of the strongly deteriorated manholes is shown.

6.3 Materials and Methods

Solid and liquid samples from different manholes throughout the whole system shown in Figure 15 were collected for further mineralogical and geochemical analyses. Gaseous samples were measured in order to determine the concentration and the stable isotopic signature of sulfur. Additionally, long term gas observations were conducted within several manholes to value total H_2S volumes.

6.4 Liquids

Liquids were sampled throughout the whole sewer system for chemical analyses. The drinking water from the surrounding region was also analyzed in order to gain reference data. On site measurements of pH, electric conductivity, O_2 concentration and redox potential were carried out. In the lab, the solutions were filtered using 0.45 µm membranes prior to alkalinity analyses by potentiometric titration with 0.005 M HCl. The concentration of dissolved components was measured by a Dionex ICS-3000 Ion Chromatograph (IC) and a PerkinElmer Optima 8300 DV inductively coupled plasma optical emission spectrometer (ICP-OES).

6.5 Solids

Deteriorated concrete was sampled from different sites and shoveled into plastic bags. The samples were dried at 40°C, and subsequently grounded for mineralogical analysis using a PANalytical X'Pert PRO diffractometer (XRD). Mineral phase identification was carried out with the PANalytical X'Pert HighScore software (version 2.2e). A hydraulic press was used to extract the pore fluids of the concrete for the above chemical analyses [4].

6.6 Gas Phase

Concentrations of gaseous H_2S, CH_4 and CO_2 within the sewer pipe atmosphere were measured using a Draeger 3000 gas monitor. Several long term gas measurements were installed in order to determine variations in the total H_2S contents.

6.7 Isotope Analyses

Gas samples of the sewer atmosphere were taken using a gas sampling tubes. The isotopic signature of carbon was directly measured. The stable sulfur isotope ratios ($^{34}S/^{32}S$) were analyzed by combustion of $BaSO_4$- or ZnS- using a Thermo Finnigan 253 mass spectrometer [5]. The $\delta^{34}S$ values, gained from $BaSO_4$ represent samples extracted from the wastewater and concrete. The $\delta^{34}S$ values obtained from ZnS reflect the signature of gaseous hydrogen sulfide (H_2S), which was captured by a 5% zinc acetate solution and consequently precipitated as ZnS. Results are given in $\delta^{34}S$-notations in ‰ relative to the Vienna-Canyon Diablo Troilite (V-CDT) standard. Figure 16 shows one of the gas traps in which H_2S was precipitated as ZnS.

Figure 16: Gas trap in a corroded manhole. This trap consists of two "Woulf'sche bottles" that contain 5% Zn-acetate solutions and an air pump. Here, H_2S reacts with the Zn-acetate to form solid ZnS.

6.8 Results and Discussion

The analyses of deteriorated concrete samples displayed mainly quartz and feldspar (albite and anorthite), which represent residuals of the siliceous aggregates of the concrete. Beside the latter phases, gypsum ($CaSO_4 \cdot 2H_2O$) and bassanite ($CaSO_4 \cdot 0.5H_2O$) were found in huge quantities. Thus, an almost complete transformation of the pristine cement matrix occurred, a process that is most likely caused by intense sulfuric acid attack. Figure 17 shows a typical composition of the deteriorated concrete within sewer manholes.

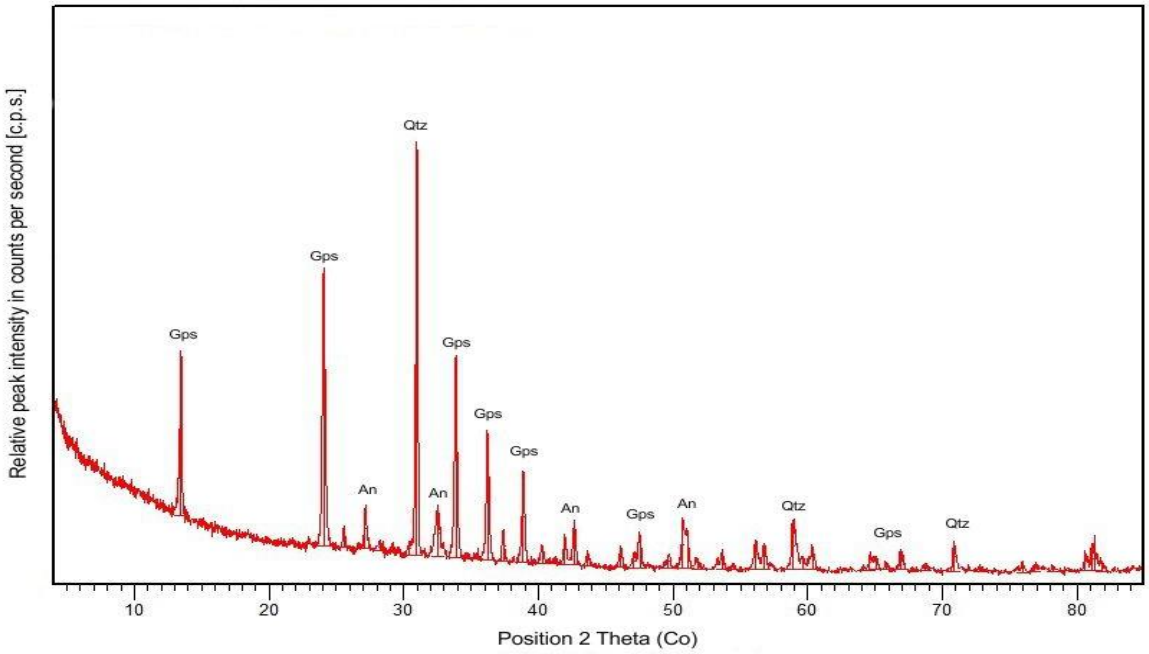

Figure 17: XRD pattern of deteriorated concrete from sewer manholes. Main component is gypsum (Gps), with aggregate residuals of quartz (Qtz) and anorthite (An).

Redox potentials from -69 down to -310 mV were measured within the first storage basin and gravity sewer, respectively. This is indicative of strictly reducing environments related to intense bacterial activity within the power main. The resultant low oxygen levels of about 0.3 mg/l in wastewater from the storage basin favored colonization of sulfate-reducing bacteria strains within the biofilm of the power main. Bacteria of the genus Desulfovibrus and Desulfobulbus that occur in such environments are known to oxidize organic matter rapidly, using sulfate as electron acceptor in the absence of oxygen or nitrogen [1, 6]. The significant decrease in sulfate concentration with flow direction, from 250 to 24 mg/l verified the reduction of sulfate to sulfide speciation by bacterial activity. Simultaneously, the H_2S level

rose up to 200 ppm in the atmosphere of the manholes. The H_2S was liberated from the wastewater into the manholes atmosphere due to changes in surrounding pressure, flow turbulences and temperature [7]. Gaseous H_2S is considered to be rapidly absorbed into the surface of concrete where it oxidizes, either by biotic or abiotic control, over a chain of complex reactions [8]. During early stages of the biogenic sulfuric acid attack, acid/base reactions of CO_2 and H_2S with the concrete resulted in the decrease of the pH from ~13.5 to ~9.5 [3]. Under such pH conditions progressive colonization of the concrete's surface by bacteria strains like Acidithiobacillus occurred. With persistent decreasing pH new strains of bacteria developed and colonized the surface of the manholes [9]. In this study, the expressed pore fluid from the corroded concrete yielded a pH value below 1, generating an extremely aggressive environment. The bacteria extracted from the deteriorated concrete were identified as Acidithiobacillus Thiooxidans and Acidithiobacillus Ferrooxidans. Those bacteria are known to be active at pH <1 if sulfate concentrations exceed 74 g/l [10]. In our samples the sulfate concentrations were up to 104 g/l. Figure 18 shows the activity of different bacteria families as a function of pH.

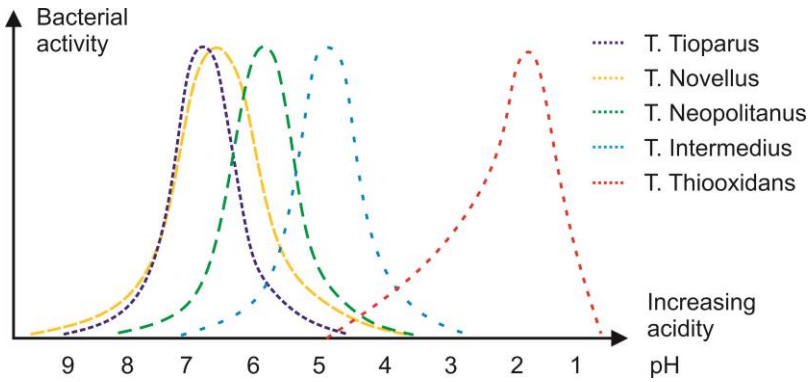

Figure 18: Distribution of bacteria families and their activities as a function of pH (modified after [9]).

Table 4: Characteristic data of fluids from the storage basins (WW-SB1), the gravity sewer (WW_GS1/2) and expressed pore fluids of the deteriorated concrete (PF).

	pH	EC [mS/cm]	Redox [mV]	O_2 [mg/l]	$H_2S_{(air)}$ [ppm]	SO_4^{2-} [mg/l]	$\delta\,^{34}S$ [‰]
WW-SB1	8	1.351	-69	0.25	bdl.	64	5.9
WW-GS1	7.4	1.298	-157	1.72	up to 44	23	7.7
WW-GS2	7.9	1.303	-188	0.68	up to 35	45	8.4
PF	0.8	10200	n.a.	n.a.	n.a.	104210	-3.4

Biogenically induced corrosion of concrete has been verified by the $\delta^{34}S$ analyses of BaSO4 and ZnS, which clearly show an isotopic fractionation between the SO_4 of wastewater and pore fluids of about 10 ‰. The latter isotopic signature was transferred to the newly formed gypsum. While we obtained $\delta^{34}S$ values between 6.0 and 8.5 ‰ for the wastewater, both the pore fluids and gypsum displayed $\delta^{34}S$ values around -3.5 ‰. In addition, a trend towards an enrichment of the heavy stables sulfur isotopes in the wastewater was recognized with flow direction, emphasizing ongoing bacterial activity.

6.9 Conclusions

The application of a multi proxy approach, including chemical, mineralogical, biological and isotopic analyses, is a very useful tool to investigate complex reactions induced by biogenic sulfuric acid attack. The deterioration of concrete in an Austrian sewer system was clearly attributed to bacteriogenically induced sulfuric acid attack and associated formation and degassing of H_2S. The observed biogenically induced isotopic fractionation of 10 ‰ $\delta^{34}S$ indicates intense colonization of different families of sulfate reducing and sulfur oxidizing bacteria. The pH values below 1 created an extremely aggressive (micro)environment within pore structures of the concrete which enhanced the decomposition of the cement paste and its alteration into gypsum. Rapid concrete corrosion is unavoidable under such conditions. The development of new strategies for sustainable remediation of the sewer system is in progress.

6.10 References

[1] H.S. Jensen, Hydrogen sulfide induced concrete corrosion of sewer networks, in: Section of Environmental Engeneering, Aalborg University, Aalborg, 2009, pp. 67.

[2] T. Hvitved-Jacobsen, J. Vollertsen, C. Yongsiri, A.H. Nielsen, S. Abdul-Talib, Sewer microbial processes, emissions and impacts, in: 3rd International Conference on Sewer Processes and Networks, Paris, 2002, pp. 1-13.

[3] A.P. Joseph, J. Keller, H. Bustamante, P.L. Bond, Surface neutralization and H_2S oxidation at early stages of sewer corrosion: Influence of temperature, relative humidity and H_2S concentration, Water Research, 46 (2012) 4235-4245.

[4] J. Tritthart, Chloride binding in cement I. Investigations to determine the composition of porewater in hardened cement, Cement and Concrete Research, 19 (1989) 586-594.

[5] J.L. Mann, R.D. Vocke, W.R. Kelly, Revised delta S-34 reference values for IAEA sulfur isotope reference materials S-2 and S-3, Rapid Commun Mass Spectrom, 23 (2009) 1116-1124.

[6] H.S. Jensen, P.N.L. Lens, J.L. Nielsen, K. Bester, A.H. Nielsen, T. Hvitved-Jacobsen, J. Vollertsen, Growth kinetics of hydrogen sulfide oxidizing bacteria in corroded concrete from sewers, Journal of Hazardous Materials, 189 (2011) 685-691.

[7] N. Matsché, E. Saracevic, F. Bertrán de Lis, L. Brooks, Korrosions- und Geruchsprobleme in der Abwasserdruckleitungen, in: Lebensministerium (Ed.), TU Wien, Vienna, 2005.

[8] R.L. Islander, J.S. Devinny, F. Mansfeld, A. Postyn, S. Hong, Microbial Ecology of Crown Corrosion in Sewers, Journal of Environmental Engineering-Asce, 117 (1991) 751-770.

[9] K.L. Scrivener, N. De Belie, Bacteriogenic Sulfuric Acid Attack of cementitious Materials in Sewage Systems, in: M. Alexander, A. Bertron, N. De Belie (Eds.) Performance of Cement-Based Materials in Aggressive Aqueous Environments, Springer, Dordrecht, 2013, pp. 305-318.

[10] E.Y. Lee, N.Y. Lee, K.S. Cho, H.W. Ryu, Removal of hydrogen sulfide by sulfate-resistant Acidithiobacillus thiooxidans AZ11, Journal of Bioscience and Bioengineering, 101 (2006) 309-314.

7 References

[1] Burian SJ, Nix, S.R., Durrans, R.E., Pitt, C.Y. The historical development of wet-weather flow management. In: Agency USEP, editor.: Nacional Service Center for Environmental Publications; 1999. p. 23.

[2] Hvitved-Jacobsen T, Vollertsen, J., Nielsen, A. H.,. Sewer processes-Microbial and Chemical Process Engineering of Sewer Networks. Second Edition ed. Padstow, Cornwall: CRC Press; 2013.

[3] Alexander M, Bertron, A., De Belie, N. Performance of Cement-Based Materials in Aggressive Aqueous Environments. Ghent: Springer; 2013.

[4] Joseph AP, Keller J, Bustamante H, Bond PL. Surface neutralization and H_2S oxidation at early stages of sewer corrosion: Influence of temperature, relative humidity and H2S concentration. Water Research. 2012;46(13):4235-45.

[5] Gutierrez O, Mohanakrishnan J, Sharma KR, Meyer RL, Keller J, Yuan Z. Evaluation of oxygen injection as a means of controlling sulfide production in a sewer system. Water Research. 2008;42(17):4549-61.

[6] Jiang G, Wightman E, Donose BC, Yuan Z, Bond PL, Keller J. The role of iron in sulfide induced corrosion of sewer concrete. Water Research. 2014;49(0):166-74.

[7] De Belie N, Monteny J, Beeldens A, Vincke E, Van Gemert D, Verstraete W. Experimental research and prediction of the effect of chemical and biogenic sulfuric acid on different types of commercially produced concrete sewer pipes. Cement and Concrete Research. 2004;34(12):2223-36.

[8] Collepardi M. A state-of-the-art review on delayed ettringite attack on concrete. Cement and Concrete Composites. 2003;25(4–5):401-7.

[9] Pavoine A, Brunetaud X, Divet L. The impact of cement parameters on Delayed Ettringite Formation. Cement and Concrete Composites. 2012;34(4):521-8.

[10] Pavoine A, Divet L, Fenouillet S. A concrete performance test for delayed ettringite formation: Part I optimisation. Cement and Concrete Research. 2006;36(12):2138-43.

[11] O'Connell M, McNally C, Richardson MG. Biochemical attack on concrete in wastewater applications: A state of the art review. Cement and Concrete Composites. 2010;32(7):479-85.

[12] Jensen HS, Lens PNL, Nielsen JL, Bester K, Nielsen AH, Hvitved-Jacobsen T, et al. Growth kinetics of hydrogen sulfide oxidizing bacteria in corroded concrete from sewers. Journal of Hazardous Materials. 2011;189(3):685-91.

[13] Hvitved-Jacobsen T, Vollertsen, J., Yongsiri, C., Nielsen, A. H., Abdul-Talib, S. . Sewer microbial processes, emission and impacts. Sewer Processes and Networks. Paris2002.

[14] Satoh H, Odagiri M, Ito T, Okabe S. Microbial community structures and in situ sulfate-reducing and sulfur-oxidizing activities in biofilms developed on mortar specimens in a corroded sewer system. Water Research. 2009;43(18):4729-39.

[15] Herisson J, Gueguen-Minerbe, M., Van Hullebusch, E. D., Chaussadent, T.,. Behaviour of different cementitious material formulations in sewer networks. Water Science and Technology. 2014;69(7):1502-8.

[16] Saracevic E. Zur Kenntnis der Schwefelwasserstoffbildung. Wien, TU Wien; 2008.

[17] Medicine USNLo. Hazardous Substance Data Bank. Rockville Pike: National Institute of Health; 2013.

[18] Hoefs J. Stable Isotopes Geochemistry. Berlin Heidelberg: Springer; 2009.

[19] Gutiérrez-Padilla MGD, Bielefeldt A, Ovtchinnikov S, Hernandez M, Silverstein J. Biogenic sulfuric acid attack on different types of commercially produced concrete sewer pipes. Cement and Concrete Research. 2010;40(2):293-301.

[20] Jensen HS. Hydrogen sulfide induced concrete corrosion of sewer networks. Aalborg, Aalborg University; 2009.

[21] Yuan H, Dangla P, Chatellier P, Chaussadent T. Degradation modelling of concrete submitted to sulfuric acid attack. Cement and Concrete Research. 2013;53(0):267-77.

[22] Olmsted FH, Hamlin, h.,. Converting portions of the Los Angeles outfall sewer into a septic tank. English News. Los Angeles1900. p. 317-8.

[23] Islander RL, Devinny, J. S., Mansfeld, F., Postyn, A., Shih, H. Microbial Ecology of crown corrosion in sewers. Journal of Environmental Engineers. 1991;117:751-70.

[24] Lee EY, Lee NY, Cho K-S, Ryu HW. Removal of hydrogen sulfide by sulfate-resistant Acidithiobacillus thiooxidans AZ11. Journal of Bioscience and Bioengineering. 2006;101(4):309-14.

[25] Nielsen AH, Vollertsen J, Jensen HS, Wium-Andersen T, Hvitved-Jacobsen T. Influence of pipe material and surfaces on sulfide related odor and corrosion in sewers. Water Research. 2008;42(15):4206-14.

[26] Herisson J, van Hullebusch ED, Moletta-Denat M, Taquet P, Chaussadent T. Toward an accelerated biodeterioration test to understand the behavior of Portland and calcium aluminate cementitious materials in sewer networks. International Biodeterioration & Biodegradation. 2013;84(0):236-43.

[27] Nielsen AH, Vollertsen, J., Jensen, H. S., Madsen, H. I., Hvitved-Jacobsen, T. Aerobic and anaerobic Transformation of sufide in a sewer system-Field study and model simulations. In: Engineering SoE, editor. Water Environment Federation's Annual Technical Exhibition and Conference. Dallas: Water Environment Foundation; 2006. p. 17.

[28] Tritthart J. Chloride binding in cement I. Investigations to determine the composition of porewater in hardened cement. Cement and Concrete Research. 1989;19(4):586-94.

[29] Starkley RL. Isolation of some bacteria which oxidize thiosulfate. Soil Science. 1935;39:197-220.

[30] Eaton AD, Clesceri, L. S., & Greenberg, A. E. . Standard Methods for Examination of water and Wastewater. In: Association APH, editor. Washington, D.C1995.

[31] Mann JL, Vocke RD, Kelly WR. Revised delta S-34 reference values for IAEA sulfur isotope reference materials S-2 and S-3. Rapid Commun Mass Spectrom. 2009;23(8):1116-24.

[32] Cappenberg TE. Interrelations between sulfate-reducing and methane-producing bacteria in bottom deposits of a fresh-water lake. Journal of Microbiology. 1974;40:285-95.

[33] Matsché N, Saracevic E, Bertrán de Lis F, Brooks L. Korrosions- und Geruchsprobleme in der Abwasserdruckleitungen. In: Lebensministerium, editor. Vienna: TU Wien; 2005.

[34] Scrivener KL, De Belie N. Bacteriogenic Sulfuric Acid Attack of cementitious Materials in Sewage Systems. In: Alexander M, Bertron A, De Belie N, editors. Performance of Cement-Based Materials in Aggressive Aqueous Environments. Dordrecht: Springer; 2013. p. 305-18.

[35] Appelo CAJ, Postma, D.,. Geochemistry, groundwater and pollution. Amsterdam: Balkema Publishers; 2005.

[36] Abdul-Talib S, Hvitved-Jacobsen, T., Vollertsen, J., Ujang, Z.,. Anoxic transformations of wastewater organic matter in sewers-process kinetics, model concept and wastewater treatment potential. Water Science and Technology. 2002;45:53-60.

[37] Herisson J, Gueguen-Minerbe, M., Van Hullebusch, E. D., Chaussadent, T.,. Developement of a reproducible, representative and accelerated biogenic corrosion test to deliver durable structures in sewer networks. In: Fentiman CH, Mangabhai, R. J., Scrivener, K. L.,, editor. Calcium Aluminates: Proceedings of the international Conference. Avignon: IHS BRE press; 2014. p. 645-58.

[38] Herisson J, Gueguen-Minerbe, M., Van Hullebusch, E. D., Chaussadent, T.,. Biogenic corrosion mechanism: Study of parameters explaining calcium aluminate cement durability. . In: Fentiman CH, Mangabhai, R. J., Scrivener, K. L.,, editor. Calcium Aluminates: Proceedings of the international Conference. Avignon: IHS BRE press; 2014. p. 633-44.

[39] Goyns AM, Alexander, M. A.,. Performance of various concretes in the Virginia experimental sewer over 20 years. In: Fentiman CH, Mangabhai, R. J., Scrivener, K. L.,, editor. Calcium Aluminates: Proceedings of the International Conference. Avignon IHS BRE press; 2014. p. 573-84.

8 List of figures

9 Appendix

9.1 Appendix A1

Table 5: Displaying amounts in wt. % of TC, TOC, SO_3 CO_2 and gypsum within concrete.

Sample ID	TC_{mean} wt.%	TOC_{mean} wt.%	TIC_{mean} wt.%	SO_3 wt.%	$[CO_2*]$ wt.%	Gypsum wt.%
GS1-M3-1s	0.17	0.17	bdl.	15.7	0.64	30.2
GS1-M5-1s	0.26	0.25	bdl.	21.9	0.94	42.2
SB2-1s	12.50	0.12	12.38	0.5	45.78	1.0
GS2-M1-2s	0.50	0.47	0.03	22.5	1.82	43.3
GS1-M4-1s	0.19	0.19	-0.01	21.6	0.68	41.7
GS2-M1-1s	0.66	0.39	0.26	26.6	2.40	51.3
GS1-M2-1s	0.42	0.41	0.01	18.6	1.55	35.8
GS2-M3-2s	0.25	0.22	0.03	20.7	0.93	39.8
GS2-M3-3s	0.27	0.25	0.02	22.2	1.00	42.7
P04_gesamt	0.78	0.33	0.44	32.8	2.84	63.2
GS1-M6-2s	0.40	0.51	-0.10	0.4	1.48	0.7
P05-1	0.33	0.35	-0.02	22.0	1.22	42.3
GS2-M2-2s	0.32	0.32	-0.01	23.4	1.16	45.1
GS2-M3-2s	0.35	0.19	0.16	16.7	1.27	32.2

bdl. [below detection limit]

9.2 Appendix A2

Table 6: Chemical composition of wastewater samples (GS1 and GS2; SB1 and SB2) as well as drinking water samples of the surrounding communities (DWP-1aq and 2aq; DWGK-1aq; DWGW-1aq). DOC denotes total dissolved organic carbon, where concentration as referred to C.

Sample ID	Na^+ mg/l	NH_4^+ mg/l	K^+ mg/l	Mg^{2+} mg/l	Ca^{2+} mg/l	Sr^{2+} mg/l	Cl^- mg/l	NO_3^- mg/l	SO_4^{2-} mg/l	PO_4^{3-} mg/l	DOC mg/l
SB1-1aq	85.4	76.9	23.1	12.9	69.1	bld.	104.2	bdl.	64.1	2.8	n.a.
SB1-4aq	72.9	85.4	21.4	13.1	83.7	0.1	90.4	bdl.	115.2	0.5	61.1
SB1-5aq	141.6	103.7	24.9	13.9	65.2	bdl.	236.6	2.6	74.3	1.8	73.0
GS1-M1-1aq	136.5	73.3	25.9	14.9	74.6	bdl.	228.4	bdl.	41.3	6.3	64.5
GS1-M3-1aq	39.6	23.6	8.6	4.8	27.3	0.2	46.3	bdl.	14.3	3.9	82.5
GS1-M3-2aq	37.3	22.7	8.3	4.9	38.0	0.2	43.8	bdl.	41.4	4.0	59.4
GS1-M3-3aq	28.6	41.3	9.6	7.9	27.7	0.2	25.9	bdl.	21.5	8.0	56.2
GS1-M3-4aq	93.4	56.8	25.2	11.2	71.5	bld.	101.6	bdl.	40.9	7.8	n.a.
GS1-M3-5aq	92.0	70.0	25.7	12.3	66.9	bld.	102.1	bdl.	23.3	14.8	n.a.
GS1-M3-7aq	68.6	50.4	18.3	10.1	79.4	0.1	87.3	bdl.	79.8	8.1	50.2
GS1-M3-8aq	67.9	50.0	18.0	9.8	70.5	0.1	86.4	bdl.	51.0	9.4	48.0
GS1-M3-9aq	70.8	58.6	18.4	10.8	73.0	0.1	94.3	bdl.	57.2	7.2	46.2
GS1-M3-10aq	138.1	74.9	23.9	15.2	73.6	bdl.	223.1	bdl.	48.8	5.3	65.0
GS1-M4-1aq	95.5	70.9	23.6	13.2	81.5	0.2	89.7	bdl.	64.4	18.6	83.7
GS1-M4-2aq	95.9	70.3	24.3	13.2	114.2	0.2	91.0	bdl.	152.4	16.8	83.0
GS1-M5-1aq	27.9	28.2	9.2	6.7	26.3	0.2	29.9	bdl.	15.4	4.0	52.4
SB2-1aq	34.8	23.5	8.2	4.8	30.3	0.2	40.2	bdl.	23.4	3.6	38.7
SB2-2aq	109.6	83.9	32.9	14.3	147.5	0.2	104.3	bdl.	249.3	15.3	83.0
GS2-M1-1aq	36.3	25.3	8.4	5.2	28.3	bdl.	43.5	bdl.	13.8	5.1	56.5
GS2-M1-2aq	77.9	68.3	24.1	17.0	77.4	bld.	85.2	bdl.	45.0	10.5	n.a.
GS2-M1-5aq	60.9	51.2	20.8	10.1	49.9	0.1	64.1	bdl.	30.8	11.3	25.5
GS2-M1-6aq	59.5	49.9	20.1	9.9	49.3	0.1	62.8	bdl.	28.7	11.2	27.5
GS2-M1-7aq	94.9	70.9	21.1	13.2	76.2	0.2	89.1	bdl.	44.5	19.0	73.2
GS2-M1-8aq	94.0	71.6	21.2	13.0	69.7	0.1	88.6	bdl.	23.8	19.4	77.3
GS2-M1-9aq	152.3	77.4	22.7	14.3	63.8	bdl.	213.9	bdl.	32.0	11.1	69.2
DWP-1aq	5.0	bdl.	1.9	12.6	91.4	0.1	6.0	14.2	50.8	bdl.	1.2
DWP-2aq	4.7	n.a.	1.7	10.5	77.8	bdl.	5.6	13.4	39.9	n.a.	n.a.
DWGK-1aq	3.1	n.a.	0.8	9.7	80.6	bdl.	7.1	8.0	19.2	n.a.	n.a.
DWGW-1aq	3.4	bdl.	0.9	35.2	82.7	n.a.	8.7	18.9	18.0	n.a.	n.a.

bdl. [below detection limit]

n.a. [not analyzed]

9.3 Appendix A3

Table 7: Chemical composition of the pore fluids, extracted from deteriorated concrete. Part 1.

Sample ID	pH	T °C	Conductivity µS/cm	Li^+ mg/l	Na^+ mg/l	NH_4^+ mg/l	K^+ mg/l
GS1-M2-PF1	2.42	21.3	5650	0.1	182	81	33
GS1-M2-PF2	3.05	21.2	4620	0.1	167	63	55
GS1-M3-PF1	2.66	21.7	8720	bdl.	109	236	186
GS1-M3-PF2	1.60	22.4	20400	0.6	103	315	163
GS1-M3-PF3	2.26	22.4	11300	0.6	100	341	194
GS1-M3-PF4	1.58	21.8	18280	0.2	75	370	111
GS1-M3-PF5	1.83	21.4	12700	0.1	59	284	108
GS2-M1-PF1	0.83	21.4	102000	7.4	2978	2994	1383
	0.94	21.4					
	1.05	21.4					
	0.97	21.4					
GS2-M1-PF2	1.04	21.7	69500	2.1	404	635	534
	1.10	21.7					
GS2-M1-PF3	0.71	22.2	100900	1.0	573	210	330
GS2-M1-PF4	0.94	22.0	66400	1.1	523	198	346

bdl. [below detection limit]

Table 8: Chemical composition of the pore fluids, extracted from deteriorated concrete. Part 2.

Sample ID	Mg^{2+} mg/l	Ca^{2+} mg/l	Sr^{2+} mg/l	F^- mg/l	Cl^- mg/l	NO_3^- mg/l	SO_4^{2-} mg/l	PO_4^{3-} mg/l
GS1-M2-PF1	52	577	3.3	bdl.	120	8.8	2719	0.9
GS1-M2-PF2	62	638	4.0	bdl.	112	11.7	2730	0.5
GS1-M3-PF1	309	542	13.7	9.2	15	52.2	7127	3.7
GS1-M3-PF2	206	621	15.0	5.2	19	45.1	9951	17.0
GS1-M3-PF3	343	508	8.1	8.1	24	45.1	9436	15.1
GS1-M3-PF4	126	494	3.5	bdl.	21	28.5	7750	7.2
GS1-M3-PF5	92	469	3.0	bdl.	17	22.4	6092	7.1
GS2-M1-PF1	4322	551	14.9	40.6	1648	6.6	104210	555.4
GS2-M1-PF2	1521	575	6.5	20.0	316	2.0	44090	345.4
GS2-M1-PF3	990	567	4.5	bdl.	376	5.3	40818	161.4
GS2-M1-PF4	931	520	8.5	bdl.	380	3.8	32717	140.8

bdl. [below detection limit]